Petrogenesis of Mediterranean lamproites and associated rocks: the role of overprinted metasomatic events in the postcollisional

Petrogenesis of Mediterranean lamproites and associated rocks: The role of overprinted metasomatic events in the post-collisional lithospheric upper mantle

Martina Casalini[1], Riccardo Avanzinelli[1,2], Simone Tommasini[1], Claudio Natali[1,3], Gianluca Bianchini[4], Dejan Prelević[5,6], Massimo Mattei[7] and Sandro Conticelli[1,3]*

[1]Dipartimento di Scienze della Terra, Università degli Studi di Firenze, Via Giorgio La Pira, 4, I-50121, Firenze, Italy

[2]CNR – Istituto di Geoscienze e Georisorse, sede secondaria di Firenze, Via Giorgio La Pira, 4, I-50121, Firenze, Italy

[3]CNR – Istituto di Geologia Ambientale e Geoingegneria, sede primaria di Montelibretti, Area della Ricerca di Roma-1, via Salaria km 29.600, I-00015, Monterotondo (RM), Italy

[4]Dipartimento di Fisica e Scienze della Terra, Università degli Studi di Ferrara, Via Giuseppe Saragat, 1, I-44122, Ferrara, Italy

[5]Institut für Geowissenschaften, Johannes Gutenberg-Universität Mainz, J.-J.- Becher-Weg 21, D-55128, Mainz, Germany

[6]Department of Petrology and Geochemistry, University of Belgrade, RS-11000, Belgrade, Serbia

[7]Dipartimento di Scienze, Università degli Studi di Roma TRE, Largo S. G. Murialdo, 1, I-00100, Roma, Italy

MC, 0000-0001-5091-4925; ST, 0000-0002-4670-5888; CN, 0000-0001-7133-2369; MM, 0000-0001-7800-8764; SC, 0000-0002-9204-0522

*Correspondence: sandro.conticelli@unifi.it, sandro.conticelli@cnr.it

Abstract: High-MgO lamproite and lamproite-like (i.e. lamprophyric) ultrapotassic rocks are recurrent in the Mediterranean and surrounding regions. They are associated in space and time with ultrapotassic shoshonites and high-K calc-alkaline rocks. This magmatism is linked with the geodynamic evolution of the westernmost sector of the Alpine–Himalayan collisional margin, which followed the closure of the Tethys Ocean. Subduction-related lamproites, lamprophyres, shoshonites and high-K calc-alkaline suites were emplaced in the Mediterranean region in the form of shallow level intrusions (e.g. plugs, dykes and laccoliths) and small volume lava flows, with very subordinate pyroclastic rocks, starting from the Oligocene, in the Western Alps (northern Italy), through the Late Miocene in Corsica (southern France) and in Murcia-Almeria (southeastern Spain), to the Plio-Pleistocene in Southern Tuscany and Northern Latium (central Italy), in the Balkan peninsula (Serbia and Macedonia) and in the Western Anatolia (Turkey). The ultrapotassic rocks are mostly lamprophyric, but olivine latitic lavas with a clear lamproitic affinity are also found, as well as dacitic to trachytic differentiated products. Lamproite-like rocks range from slightly silica under-saturated to silica over-saturated composition, have relatively low Al_2O_3, CaO and Na_2O contents, resulting in plagioclase-free parageneses, and consist of abundant K-feldspar, phlogopite, diopsidic clinopyroxene and highly forsteritic olivine. Leucite is generally absent, and it is rarely found only in the groundmasses of Spanish lamproites. Mediterranean lamproites and associated rocks share an extreme enrichment in many incompatible trace elements and depletion in High Field Strength Elements and high, and positively correlated Th/La and Sm/La ratios. They have radiogenic Sr and unradiogenic Nd isotope compositions, high ^{207}Pb over ^{206}Pb and high time-integrated $^{232}Th/^{238}U$. Their composition requires an originally depleted lithospheric mantle source metasomatized by at least two different agents: (1) a high Th/La and Sm/La (i.e. SALATHO) component deriving from lawsonite-bearing, ancient crustal domains likely hosted in mélanges formed during the diachronous collision of the northward drifting continental slivers from Gondwana; (2) a K-rich component derived from a recent subduction and recycling of siliciclastic sediments. These metasomatic melts produced a lithospheric mantle source characterized by network of felsic and phlogopite-rich veins, respectively. Geothermal readjustment during post-collisional events induced progressive melting of the different types of veins and the surrounding peridotite generating the entire compositional spectrum of the observed magmas. In this complex scenario, orogenic Mediterranean lamproites represent rocks that characterize areas that were affected by multiple Wilson cycles, as observed in the Alpine–Himalayan Realm.

Supplementary material: All the data used in the figures are available at https://doi.org/10.6084/m9.figshare.c.5414418

From: Krmíček, L. and Chalapathi Rao, N. V. (eds) *Lamprophyres, Lamproites and Related Rocks: Tracers to Supercontinent Cycles and Metallogenesis*. Geological Society, London, Special Publications, **513**, https://doi.org/10.1144/SP513-2021-36

Lamproites are rare and exotic ultrapotassic igneous rocks ($K_2O > 3$ wt.%, with $K_2O/Na_2O > 2$; Foley *et al.* 1987) showing peculiar geochemical and isotopic compositions. They have mafic to ultramafic character (Mg-# = 100 $Mg/(Mg + Fe) > 60$), and high compatible trace element contents (Mitchell and Bergman 1991). These characteristics combined with the occurrence of euhedral to skeletal, highly forsteritic, liquidus olivine, support that lamproite magmas were in equilibrium with their mantle source in spite of their extraordinary enrichment in incompatible trace elements (Mitchell and Bergman 1991; Conticelli *et al.* 1992, 2007, 2009; Prelević *et al.* 2005, 2012, 2015; Davies *et al.* 2006; Prelević and Foley 2007; Tommasini *et al.* 2011; Ammannati *et al.* 2016; Mitchell 2020).

The extreme enrichment in K_2O and incompatible trace elements of lamproites was shown to be not dependent upon crustal contamination during magma ascent to surface, which was instead demonstrated to be negligible (Conticelli 1998; Murphy *et al.* 2002; Prelević *et al.* 2004). Hence, it is thought that such an enrichment is a primary feature of their mantle source (Peccerillo *et al.* 1988; Conticelli and Peccerillo 1992; Conticelli *et al.* 2002, 2009, 2015; Davies *et al.* 2006; Peccerillo and Martinotti 2006; Duggen *et al.* 2008; Prelević *et al.* 2008; Avanzinelli *et al.* 2009; Krmíček *et al.* 2016, 2020).

Occurrences of lamproites are described in both anorogenic (i.e. within-plate) and orogenic, post-collisional tectonic settings, rarely within ancient cratons, more often in areas of thickened crust at cratonal margins, which experienced one or several episodes of compression or post-collisional collapse (Mitchell and Bergman 1991; Mitchell 2020).

Within-plate and post-collisional lamproites show a distinct distribution of radiogenic Sr and Nd, with the former characterized by comparably low Sr and Nd isotope ratios, and the latter by high radiogenic Sr and unradiogenic Nd isotopes (e.g. McCulloch *et al.* 1983; Nelson *et al.* 1986; Nelson 1989, 1992; Irving and Kuehner 1998; Turner *et al.* 1999; Francalanci *et al.* 2000; Conticelli *et al.* 2007, 2009; Prelević *et al.* 2008, 2010). Both within-plate and post-collisional lamproites are characterized by high $\delta^{18}O$ (6–13‰; Taylor *et al.* 1984; Barnekow *et al.* 1998; Benito *et al.* 1999; Barnekow 2000; Mirnejad and Bell 2006), a characteristic that, for post-orogenic ones, was argued to be related with recycled crustal-derived heavy oxygen within the mantle (Dallai *et al.* 2019; Avanzinelli *et al.* 2020).

To our knowledge, recent (<30 Ma) orogenic lamproites are mainly concentrated in Europe and in the Tibet region, along the Alpine–Himalayan belt. Lamproitic magmatism is relatively common in the Mediterranean area (Fig. 1) and it is considered to be the consequence of the post-collisional events, which took place in the orogenic belt originated from the Mesozoic and Paleogene convergence between Africa and Eurasia (Tommasini *et al.* 2011). In such a post-collisional setting lamproites are frequently intimately associated with calc-alkaline lamprophyric, shoshonitic and high-K calc-alkaline rocks (Conticelli *et al.* 1992, 2007, 2009, 2011, 2013, 2015; Prelević *et al.* 2004, 2005, 2012, 2015; Peccerillo and Martinotti 2006; Prelević and Foley 2007; Owen 2008; Avanzinelli *et al.* 2009).

In this paper we describe the geochemical and isotopic data available on the orogenic group of Mediterranean lamproites (Fig. 1), including the occurrences from Murcia (SW Spain), Western Alps (NW Italy), Corsica (France), Tuscany (central Italy), Balkan Peninsula (Serbia–Macedonia) and Western Anatolia (Turkey), and their associated shoshonitic and calc-alkaline rocks. The discussion will be framed on the origin of the subduction-related signature of their mantle source and on the nature of the metasomatic agents and recycled crustal materials. The geochemical and isotopic data are supplemented with chemical data on rock-forming minerals, as well as data on mantle xenoliths possibly representing proxies for the sources of such peculiar magmas. All together the genesis of lamproitic magmas is discussed in the frame of the geodynamic evolution of the region.

Lamproites, lamprophyres and associated rocks

Due to their exotic rock-forming minerals lamproites were classified with a large variety of now obscure names such as wyomingite, orendite, madupite, jumillite, cancalite, fortunite, verite, cedricite, fitzroyite, etc. (De Yarza 1895; Cross 1897; Osann 1906; Wade and Prider 1940) but we prefer to use the general term lamproite according to the classification suggested by Foley *et al.* (1987).

Lamproites are Mg-rich alkaline ultrapotassic volcanic to hypo-abyssal rocks (Foley and Venturelli 1989; Mitchell 2020). They are characterized by relatively low Al_2O_3, FeO_{Tot}, CaO and Na_2O counterbalanced by extremely high MgO, and extremely variable silica contents, the latter ranging from basic to intermediate compositions. Lamproites are generally silica-saturated, plagioclase-free rocks, consisting of highly forsteritic olivine, chromian spinel, Al-poor clinopyroxene, K-richterite, sanidine, picroilmenite and apatite. Leucite is rarely found in minor silica-undersaturated lamproites.

Lamprophyre is an important category of hypabyssal rocks (Rock 1987), whose name is based on mineralogical criteria, such as the type of occurring feldspar and possible amphibole; minette, spessartite and kersantite are the rock names according to the mineralogical classification. They are potassic to

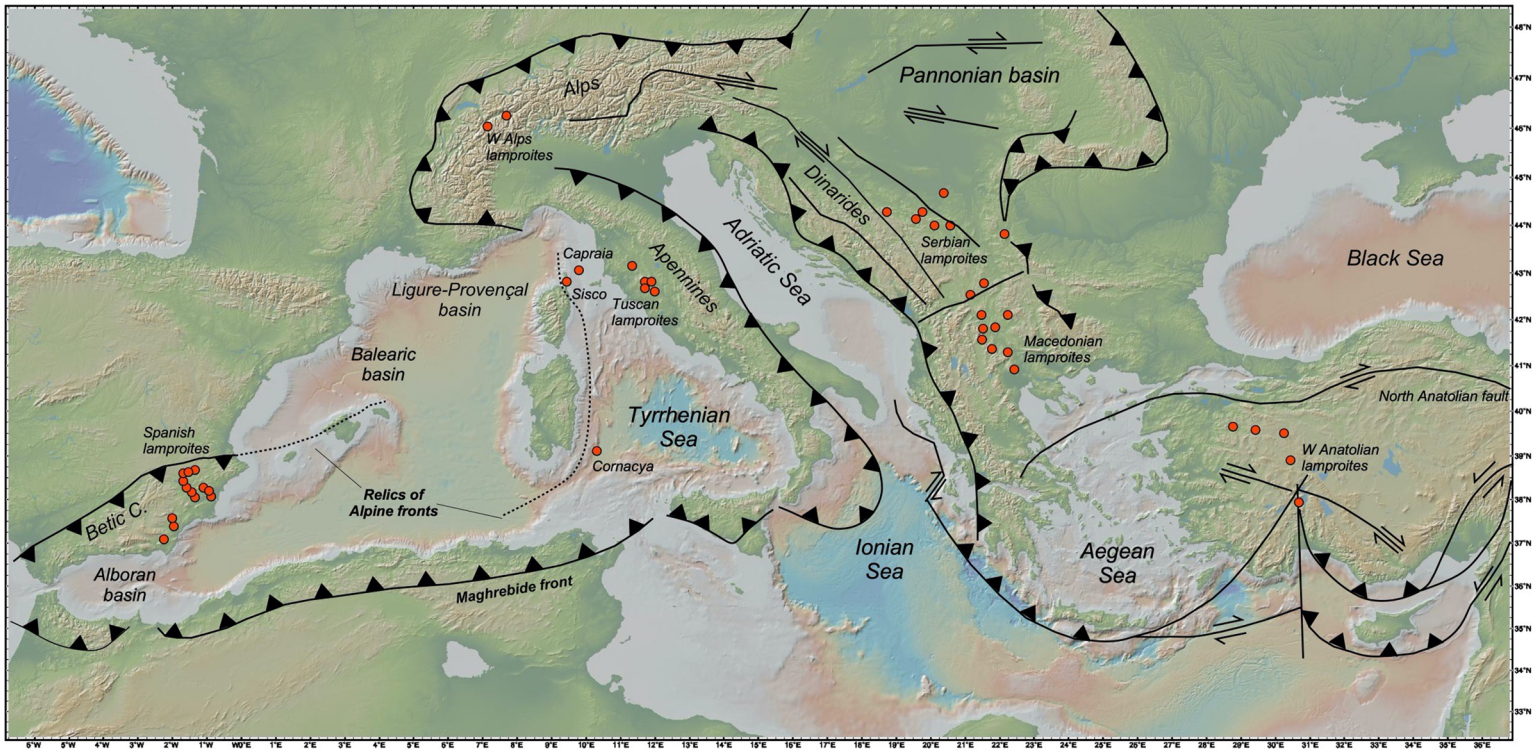

Fig. 1. Simplified tectonic map of the Mediterranean area showing the distribution of lamproites (red dots). Major faults are indicated by black lines. The present Apennine–Maghrebian compression front and the Alpine collision zone are also indicated (base GeoMapApp, http://www.geomapapp.com).

ultrapotassic with higher alumina and lime with respect to lamproites, but in some cases they are chemically very similar to lamproitic to ultrapotassic shoshonitic rocks (Foley *et al.* 1987).

Shoshonite is a group of igneous rocks ranging from mildly enriched in potassium to ultrapotassic, with variable silica saturation. The rock types range from potassic trachybasalt (shoshonitic basalt) to trachyte, passing through shoshonite *sensu stricto* and latite. These rocks have variable enrichment in K_2O in the most primitive terms.

High-K calc-alkaline and calc-alkaline rocks are defined on the basis of K_2O contents with respect to silica (Wheller *et al.* 1987). They match the chemical and mineralogical parameters provided by Arculus (2003). They are sub-alkaline with terms ranging from basalts to rhyolites, passing through basaltic andesite, andesite and dacite. The prefix high-K is added when needed.

Geodynamic framework of the Mediterranean region

The Circum-Mediterranean region experienced a long-term evolution including oceanic subduction and continental collision processes related to the convergence between Africa–Arabia and Eurasia plates (McKenzie 1970; Dewey *et al.* 1989; Faccenna *et al.* 2004). Multiple convergences and collisions among Africa–Arabia and Eurasia plates caused the diachronous closure of the Paleo-Tethys and Neo-Tethys oceans, and the progressive accretion of peri-Gondwana blocks to the southern margin of the Eurasian plate (Sengör 1979; Allen and Armstrong 2008; Zanchetta *et al.* 2013). Subduction and collisional processes caused the formation of different orogenic belts, including the Late Triassic–early Jurassic Cimmerian Orogeny in Turkey and Iran (Stocklin 1974; Zanchi *et al.* 2009), and the almost continuous Alpine orogenic belt that extends from the Gibraltar Arc, which is the westernmost segment of the Alpine–Mediterranean Belt, to western Anatolia in Turkey (Fig. 1). Interestingly, within the whole Alpine–Mediterranean Belt, vestiges of older (Paleozoic) orogenic cycles are well represented and testify the polycyclic geodynamic evolution of the area (Von Raumer *et al.* 2002).

During this long-lasting process, the tectonic evolution of the convergent margins was mainly controlled by the geometry and nature of the convergent plates, which were characterized by the presence of continental promontories, such as the Arabian plate and the Adriatic promontory of Africa which underwent an early collisional stage, interleaved with areas where subduction of the oceanic lithosphere is still going on (e.g. Calabrian, Aegean and Ciprus arcs). This heterogeneity in the subduction system was responsible for the complex evolution of the upper plate system, which was characterized by the presence of arcuate orogenic systems, back-arc basins (Alboran, Liguro-Provençal, Tyrrhenian, Aegean Sea basins) and kinematically independent crustal blocks (e.g. Corsica–Sardinia, Anatolia), which developed as a consequence of roll-back in the subducting slab and lateral extrusion of pieces of continental lithosphere (McKenzie 1970; Horvath and Berckheimer 1982; Dewey *et al.* 1989). This complexity is also responsible for the large variability in metasomatic processes and magmatism occurred in the Mediterranean region.

Mediterranean lamproites were formed since the Oligocene (Western Alps, NW Vardar zone), to the Miocene (Corsica, Murcia–Almeria, Western Anatolia), the Mio-Pliocene (Serbia, southern Vardar zone) and the Plio-Pleistocene (Tuscany) (Conticelli *et al.* 1992; Benito *et al.* 1999; Prelević *et al.* 2004, 2005, 2008; Kuiper *et al.* 2006; Pérez-Valera *et al.* 2013; and references reported in these papers) (Fig. 1).

Western Mediterranean

The western Mediterranean area was exposed to multiple orogenic episodes that left inheritance in the subsequent, more recent geodynamic evolution (Ribeiro *et al.* 2007). A large number of palaeotectonic reconstructions proposed that during the Oligocene (about 30 Ma) the boundary between Africa and Eurasian plates in the western Mediterranean area was characterized by the presence of a convergent margin with almost continuous northward subduction of the African plate from Gibraltar to the Apennine chain (Faccenna *et al.* 2004) (Fig. 1). The subduction of the African plate evolved with a backward motion of the subduction trench, enhanced by the fragmentation of the subducting slab which brought about the progressive formation of the Calabrian Arc and Gibraltar. The former is associated with the opening of the Liguro-Provençal (30–16 Ma) and Tyrrhenian (12–1 Ma) back arc basins, the latter is associated to the opening of the Alboran back arc basin (Lower Miocene) (Fig. 1) (Lonergan and White 1997; Faccenna *et al.* 2004, 2014; Mattei *et al.* 2006; Cifelli *et al.* 2008). During the Late Miocene, the Gibraltar region experienced drastic modification of the tectonic regime, then the whole Betic-Rif and the Alboran Sea Basin underwent a complex pattern of compressional and strike-slip tectonics which, in some cases, inverted previous extensional structures (Watts *et al.* 1993; Comas *et al.* 1999). Volcanism accompanied and post-dated Neogene extension, with arc-tholeiitic, calc-alkaline, shoshonitic and ultrapotassic volcanism scattered across the eastern sector of Alboran Sea and Betic-Rif chain (Venturelli *et al.* 1984*a*; Duggen *et al.* 2005, 2008; Mattei *et al.* 2014).

The Miocene-to-Present formation of the Apennine chain was coeval with the fast opening of the Liguro-Provençal (first) and the Tyrrhenian back arc (later) basins following the southeastward retreat of a NW–west dipping Ionian/Adriatic slab (Malinverno and Ryan 1986; Royden *et al.* 1987; Faccenna *et al.* 2004; Cifelli *et al.* 2007). Linked to this geodynamic evolution are the lamproite and associated volcanic rocks of Corsica and the northern Tyrrhenian Sea, which migrated regularly with time, from Miocene to Pleistocene following the Adriatic slab roll back, to Tuscany, on the Italian Peninsula (Faccenna *et al.* 2014).

Western Alps

The western Alps are a continuation of the same convergent system but with an opposite polarity of the subducted plate, the direction of which reversed in the Ligurian area (Pfiffner 2021). They also originated from Africa and Eurasia convergence, from the late Cretaceous onward, causing the closure of the Ligurian–Piedmont and Valais oceans and the subsequent collision between the Adriatic promontory and the Eurasian plate (Dercourt *et al.* 1986; Stampfli *et al.* 2001). Collision was accommodated by crustal stacking and subduction of continental material as attested by the presence of ultra-high pressure rocks in the Dora Maira massif (Chopin 1984; Schreyer *et al.* 1987). Rare hypabyssal bodies and volcanic rocks were emplaced shortly after the climax of the Alpine orogenesis (Dal Piaz *et al.* 1979; Venturelli *et al.* 1984*b*; Callegari *et al.* 2004). It appears clear that this 'alpine' geodynamic phase was influenced by pre-alpine lineaments that left their inheritance on palaeogeographic domains (Festa *et al.* 2020).

Dinarides

The Dinarides orogenic system represents the northern part of a continuous belt extending from the eastern Alps to southern Greece, including the Albanides and Hellenides orogens (Fig. 1). The Dinaride geodynamic evolution records a long-lasting history of orogenic deformation at least from the Paleozoic (Ilic *et al.* 2005), which continued during the Early–Middle Jurassic and is still going on. The geodynamics of the internal Dinarides was controlled by the presence of oceanic basins (including the Alpine Tethys and Neo-Tethys) opened during the break-up of Pangea (Stampfli *et al.* 2001) with episodes of intra-oceanic subduction represented in local ophiolites (Bortolotti *et al.* 2013). The Neo-Tethys opened during Triassic and Early to Mid-Jurassic times, whilst the Alpine Tethys started to open during the Mid-Jurassic and was contemporaneous with partial closure of the western Neo-Tethys and the obduction of the Eastern and Western Vardar Ophiolitic Units on top of the Adriatic passive margin (Schmid *et al.* 2004). The external part of the Dinarides is formed by shallow marine and basinal sedimentary units deriving from the deformation of the Adriatic passive margin, which was progressively involved in the Dinaride orogenic system as a consequence of the eastward subduction of the Adriatic margin. This orogenic deformation is still active along the coastal sector of the Dinaride and Albanide orogenic systems, as testified by the strong seismicity of the area.

Western Anatolia

Western Anatolia consists of different continental units, derived from Laurentia and Gondwana margins, originally separated by the Paleo-Tethys and Neo-Tethys oceans and eventually amalgamated during the Alpine Orogeny (Robertson *et al.* 2012). The Pontide units, which outcrop in the northern sector of the Anatolia region, show a Laurasian affinity and were deformed by the Variscan and Cimmerian orogenies, showing analogies with the pre-Alpine geological history of many European zones (Okay *et al.* 2006). The Paleo-Tethys and Neo-Tethys sutures separate the Pontides units from the the Anatolide–Tauride realms, showing Gondwana affinities and lacking evidence of Variscan and Cimmerian orogenesis (Okay 2008). The closure of these Mesozoic oceans was followed by the progressive subduction, along the southern margin of Anatolia, of the Ionian lithosphere. As a consequence, the entire Western Anatolia region today is located in the upper plate of the Aegean subduction system, where the Ionian oceanic lithosphere is subducting northeastward underneath the southern margin of the Eurasian plate. This active subducting slab is limited to the NE by the Kefalonia fault, which separates the Adriatic continental lithosphere, to the north, from the oceanic Ionian lithosphere to the south. Slab roll-back during the last 30–35 Ma has been responsible for extensional back-arc opening in the Aegean Sea and of the progressive curvature of the Aegean Arc (Kissel and Laj 1988), which caused the exhumation of high pressure/low temperature metamorphic cores (Jolivet and Brun 2010).

Occurrence and petrologic, geochemical and isotopic characteristics of Mediterranean lamproites

Mediterranean lamproites occur in a narrow belt (Fig. 1) composed of small-volume hypo-abyssal (e.g. plugs, laccoliths, lopoliths and dykes) and lava flows from the Murcia–Almeria region (southeastern Spain), through the Italian and French Alpine

chain (Western Alps and Corsica, respectively), and the northern edge of the Apennine chain (Tuscany), to the Dinarides (Serbia–Macedonia) and Taurides (Western Anatolia). The Mediterranean region represents the westernmost segment of the major collisional system that led to the formation of the Alpine–Himalayan Orogeny. Overall, the entire set of Alpine–Himalayan lamproites were referred to as Tethyan Realm Lamproites (i.e. Tommasini *et al.* 2011).

Murcia–Almeria is the westernmost and largest magmatic province among those including Tethyan Realm Lamproites (Fig. 1). Lamproite-like ultrapotassic rocks (Murcia) are associated to shoshonitic to high-K calc-alkaline magmatism (Cabo de Gata, Mazàron). Two-pyroxene calc-alkaline rocks, found exclusively at Capo de Gata (Almeria), high-K calc-alkaline and shoshonites, found along the Murcia–Almeria coast (Mazàron) are among the oldest volcanic products of the region (13.4–6.8 Ma), whilst Murcia lamproites were emplaced during the last phases of the volcanic activity (8.1–6.4 Ma) (Turner *et al.* 1999; Duggen *et al.* 2005; Kuiper *et al.* 2006; Pérez-Valera *et al.* 2013; Mattei *et al.* 2014). Murcia lamproites show the largest compositional variability of any region of lamproites in the whole Mediterranean (Fig. 2). Among the associated volcanic rocks shoshonites are rare, most of them straddling the boundary between shoshonitic and high-K calc-alkaline fields in the K_2O v. SiO_2 diagram (Fig. 2). However, some shoshonites plot along a trend at very high K_2O contents, connecting with lamproites. Intermediate to strongly differentiated calc-alkaline rocks are abundantly found in Cabo de Gata volcanic field (Mattei *et al.* 2014).

The Western Alps post-collisional lamproite and related shoshonitic to high-K calc-alkaline igneous rocks are found within a restricted area in the internal zone of the northwestern Alps (Venturelli *et al.* 1984*b*; Peccerillo and Martinotti 2006; Owen 2008; Conticelli *et al.* 2009; Casalini 2018). The age of this magmatism was found to be within the range 34–30 Ma (Krummenacher and Evernden 1960; Carraro and Ferrara 1978; Hunziker 1974), which is coeval with the peak of post-collisional magmatism of the entire Alps (Von Blanckenburg *et al.* 1998). Lamproitic-like plagioclase-free rocks were classified by Owen (2008) as minette due to their micaceous appearance; groundmasses have intersertal textures with phlogopite, clinopyroxene and K-feldspar, accompanied by minor altered olivine and riebeckite–arfvedsonite amphibole. Shoshonitic to high-K calc-alkaline plagioclase-bearing rocks (kersantite to spessartite) are found associated in space and time with ultrapotassic rocks. Strictly speaking, these rocks should be classified as lamprophyres on a mineralogical basis (Owen 2008), but we prefer to use the term lamproite on the basis of the chemical classification suggested by Foley *et al.* (1987). In the SiO_2–K_2O diagram, Western Alp lamproites plot close to the lamproitic samples from Corsica and Murcia–Almeria (Fig. 2) overlapping at the low-silica end those from Corsica (Fig. 2).

Miocene lamproitic, shoshonitic and high-K calc-alkaline igneous rocks association is found along the eastern margin of the Sardinia–Corsica micro-plate (Fig. 1). Lamproites are restricted to the northeastern portion of the Corsica Island, in the form of a sill intruded into the Alpine terranes belonging to the 'Schistes Lustrés' (Wagner and Velde 1986; Peccerillo *et al.* 1988; Conticelli *et al.* 2009); shoshonitic to high-K calc-alkaline subvolcanic to volcanic rocks are found a few kilometres offshore from Sardinia and Corsica in the locality of Sisco, at Sarcya seamount (Cornacya) and Capraia Island, respectively (Mascle *et al.* 2001; Chelazzi *et al.* 2006; Conticelli *et al.* 2007; Gasparon *et al.* 2009; Avanzinelli *et al.* 2009). The Sisco lamproites have an age of 14.6 Ma (Civetta *et al.* 1978), whilst the shoshonitic samples from Cornacya were erupted at 12.6 Ma (Mascle *et al.* 2001). The Capraia high-K calc-alkaline rocks were erupted between 7.8 and 7.2 Ma, with a small cinder cone at Punta dello Zenobito erupted at 4.8 Ma (Gasparon *et al.* 2009). The Sisco lamproite is a leucite- and plagioclase-free ultrapotassic rock with intersertal texture and a parageneses made of phlogopite, clinopyroxene, olivine, sanidine and K-richterite associated to subordinate abundance of chromian spinel, ilmenite, pseudobrookite and priderite (Wagner and Velde 1986). Shoshonitic (Cornacya) and high-K calc-alkaline rocks (Capraia) range from shoshonites, to olivine latites, trachytes, high-K andesites, trachy-dacites and rhyolites and they are characterized by the occurrence of modal plagioclase, with sanidine and hornblende restricted to the most differentiated rocks (Mascle *et al.* 2001; Gagnevin *et al.* 2007; Conticelli *et al.* 2015). The Sisco lamproites show a peralkaline index >1, and the highest K_2O and the lowest Al_2O_3, respectively, among the whole Central Mediterranean lamproites (Prelević *et al.* 2008; Conticelli *et al.* 2009).

The Plio-Pleistocene Tuscan lamproite-like and associated rocks are found in Central Italy (Fig. 1) and they are emplaced as (1) phlogopite-bearing shallow level intrusive bodies (i.e. Orciatico and Montecatini Val di Cecina) that are 4.2 and 4.1 Ma in age (Borsi *et al.* 1967; Conticelli *et al.* 1992), and (2) olivine-bearing lava flows (i.e. Torre Alfina and Monte Cimino) erupted between 0.9 and 0.8 Ma (Nicoletti 1969; Nicoletti *et al.* 1981; Borghetti *et al.* 1981), with shoshonites to high-K calc-alkaline rocks with variable ages between 5.8 Ma (Elba Island dyke) and 1.1 Ma (Barberi *et al.* 1971; Pasquaré *et al.* 1983; D'Orazio *et al.*

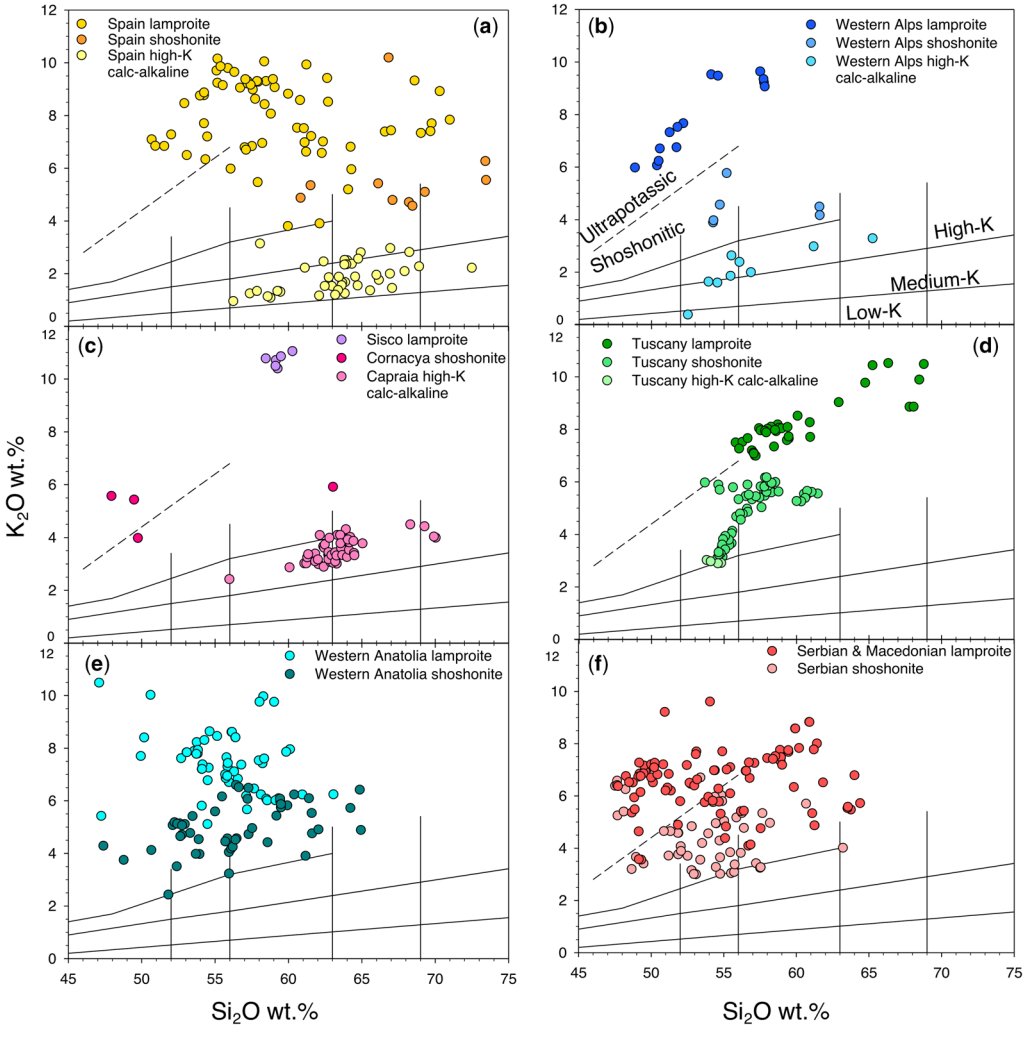

Fig. 2. K_2O v. SiO_2 classification diagram (Ewart 1982). Dashed line represents the divide of Wheller *et al.* (1987) between shoshonite and leucitite but we prefer to use the term ultrapotassic since leucite is absent in the Mediterranean orogenic lamproites. For each location (a–f) lamproite rocks are compared to associated shoshonitic and high-K calc-alkaline rocks. The data are taken from the literature and the complete dataset is available as Supplementary Material (Table S1). (**a**) Spain: Venturelli *et al.* 1984*a*; Nelson *et al.* 1986; Benito *et al.* 1999; Turner *et al.* 1999; Prelević *et al.* 2008; Conticelli *et al.* 2009; Pérez-Valera *et al.* 2013; Mattei *et al.* 2014. (**b**) Western Alps: Owen 2008; Prelević *et al.* 2008; Conticelli *et al.* 2009; Casalini 2018. (**c**) Corsica, Cornacya and Capraia: Peccerillo *et al.* 1988; Mascle *et al.* 2001; Chelazzi *et al.* 2006; Conticelli *et al.* 2009, author's unpublished data. (**d**) Tuscany: Peccerillo *et al.* 1988; Conticelli 1998; Conticelli *et al.* 1992, 2011, 2013; Perini *et al.* 2003; Prelević *et al.* 2008; Casalini *et al.* 2019. (**e**) Serbia and Macedonia: Cvetković *et al.* 2004*a*; Prelević *et al.* 2004, 2005, 2008, 2010; Altherr *et al.* 2004. (**f**) Western Anatolia: Akal 2008; Ersoy and Helvaci 2007; Francalanci *et al.* 2000; Prelević *et al.* 2012, 2015.

1991; Conticelli *et al.* 2001). Plagioclase-free lamproite-like rocks of Tuscany (Italy) have a peralkaline index <1, but their mineralogy is typical of lamproite-like rocks (Wagner and Velde 1986; Conticelli *et al.* 1992; Conticelli 1998). Olivine is commonly the only phenocryst phase and usually encloses Al-poor and Cr-rich euhedral spinel. Phlogopite and Al-poor clinopyroxene are the most abundant phases in the groundmass; sanidine is ubiquitous. Lamproite-like rocks from Tuscany show

lower K_2O at comparable SiO_2 contents with respect to similar Mediterranean rocks (Fig. 2). Shoshonites are abundant showing the most mafic compositions among the Mediterranean shoshonites (Perini *et al.* 2003; Conticelli *et al.* 2011, 2013).

In the Balkan region, lamproite magmatism recurs in two areas (Fig. 1) and is diachronous in time (Altherr *et al.* 2004; Prelević *et al.* 2005, 2007, 2008). In the northern part of the province (Serbia), a broad spectrum of ultrapotassic rocks with lamproitic affinity (i.e. lamproites and minette) was emplaced around 35 Ma in several localities of the Vardar ophiolitic suture zone. After about 15 Myr magmatism shifted southward producing plugs and flows with kamafugitic affinity (i.e. olivine leucitite, leucite basanite and ankaratrites; Prelević *et al.* 2005) were emplaced in the southern–western part of the Serbian Dinarides (Prelević *et al.* 2005, 2007). The second Balkan sub-province occurs in Macedonia and in a few southern Serbia localities. Here, more than 20 distinct lamproitic volcanic centres with Pliocene Age (e.g. 6.6–1.5 Ma; Terzić and Svešnjikova 1991; Cvetković *et al.* 2004*a*; Yanev *et al.* 2008) occur as cinder cones, lava flows and plugs. Despite the significant age difference, the youngest lamproites cannot be distinguished from the older Balkan lamproitic rocks in terms of mineralogy or geochemistry (Prelević *et al.* 2007). In between the two lamproitic magmatic events, minor high-K calc-alkaline and abundant shoshonitic rocks were also emplaced (Fig. 2).

In western Anatolia Tertiary lamproitic rocks were produced along the Hellenic and Cyprus arc (Fig. 1), at the eastern end of the Aegean volcanic arc, resulting from the northward subduction of the African Plate beneath the Aegean (Doglioni *et al.* 2002; Innocenti *et al.* 2005). Here, volcanism started with calc-alkaline products in the Eocene, partially coeval with Aegean volcanism, and continued during the Miocene with shoshonitic to lamproitic products (e.g. Prelević *et al.* 2007, 2012). Another occurrence of ultrapotassic volcanics is located slightly to the south in the north–south trending Kýrka-Afyon-Isparta volcanic province (Francalanci *et al.* 2000; Akal 2008). This province was emplaced in three steps that exhibit southward younging from Kýrka (21–17 Ma) to Afyon (14–8 Ma) and Isparta (4.7–4.0 Ma). These rocks have ultrapotassic to potassic character (i.e. shoshonitic; Fig. 2). Among lamproites, the ultrapotassic terms, Kýrka and Afyon show a clear orogenic signature whilst Isparta displays a within-plate signature (Francalanci *et al.* 2000; Akal 2008).

Trace element distribution

Mediterranean lamproites usually have high contents of compatible trace elements (e.g. Ni > 200 ppm and Cr > 500 ppm) coupled with significant enrichments in incompatible elements and rare earth elements (REEs), with some large ion lithophile element (LILE, e.g. Rb, Cs) concentrations up to four orders of magnitude higher than those of the Primitive Mantle (Fig. 3). In addition, they display a notable depletion in high field strength elements (HFSEs, e.g. Nb, Ta), resulting in high LILE/HFSE ratios, which, along with Pb peaks, are clearly indicative of a subduction-related signature.

Despite their general crustal-like patterns, K and highly incompatible elements (e.g. Rb, Ba, Th and U) in orogenic lamproites have on average different distributions with respect to the present-day upper crust (Rudnick and Gao 2003) and Global Subducting Sediment (GLOSS, Plank and Langmuir 1998). Indeed, a distinctive signature of Mediterranean and, more in general, of Tethyan Realm Lamproites is their relative depletion in Ba and Sr with respect to Rb and Th (Tommasini *et al.* 2011). Ratios between the aforementioned elements (Fig. 4) also help in distinguishing orogenic from anorogenic lamproites. Indeed, orogenic lamproites show higher Rb/Sr coupled with lower Ba/Rb than anorogenic ones (Fig. 4a), suggesting an important role for bulk melting of phlogopite and amphibole, respectively, in their mantle sources.

The extreme enrichment of Th (up to >200 ppm) in all the orogenic, Tethyian Realm Lamproites results in high Th/U, well beyond the Th/U ratio of *c.* 4 of the crust and most mantle-derived igneous rocks (Fig. 4b) (Plank and Langmuir 1998; Rudnick and Gao 2003). The high Th content entails one of the most striking features of these rocks, that is the positive correlation between Th/La and Sm/La (Fig. 4d). These key ratios are instead not correlated with K_2O (e.g. Fig. 4c).

This characteristic is due, beside the extreme Th content, also to the slightly downward convex light (L) REE patterns (Conticelli *et al.* 1992, 2007, 2009, 2015). The positive correlation between Th/La and Sm/La observed by Tommasini *et al.* (2011), actually represents a sort of paradox when compared to subduction-related magmas worldwide. Indeed, Plank (2005) showed that typical volcanic arc magmas exhibit a negative correlation on Th/La v. Sm/La, arguing for mixing between depleted mantle (at low Th/La and high Sm/La) and subduction-related components (i.e. end-members), the latter derived from melts of recycled sediments characterized by relatively high Th/La (*c.* 0.5–0.7) and low Sm/La (*c.* 0.1). The composition of Tethyan Realm Lamproites fall along the trend between the recycled sediment end-member (Plank 2005) and another one at high Th/La and Sm/La (up to 2.2 and 0.4, respectively, see also Fig. 4d), termed SALATHO (high Sm, La and Th; Tommasini *et al.* 2011), which is difficult to explain in terms of notional mantle and crustal reservoirs.

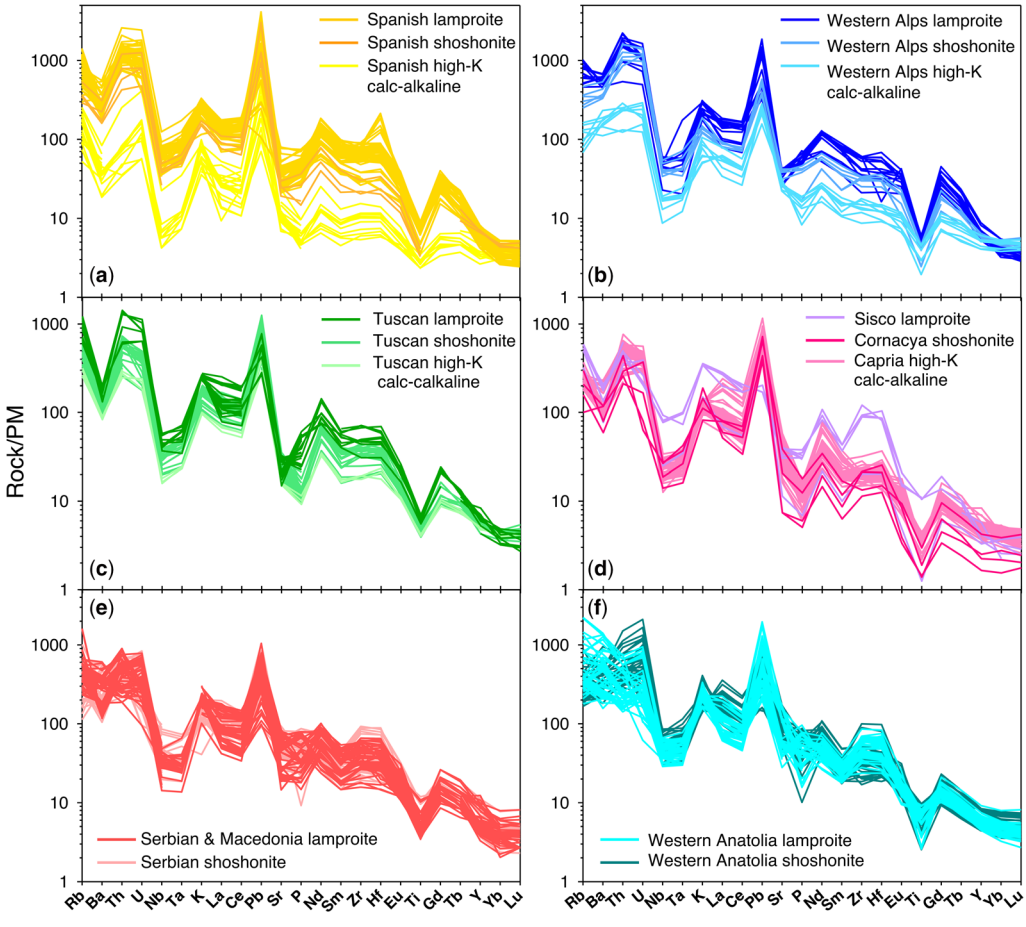

Fig. 3. Primitive mantle normalized (Sun and McDonough 1989) incompatible trace element patterns of orogenic lamproites and associated shoshonitic and high-K calc-alkaline rocks (**a–f**). Data source as in Figure 2 (Table S1).

Radiogenic isotopes

Mediterranean lamproites show extreme variability in their radiogenic isotope composition, much more than anorogenic lamproites and other terrestrial mantle-derived magmas (Conticelli and Peccerillo 1992; Conticelli *et al.* 1992, 2002, 2007, 2009, 2015; Prelević *et al.* 2005, 2007, 2008, 2010, 2012, 2015). All lamproites lie in the enriched quadrant of the Sr–Nd isotope diagram (Fig. 5a), with respect to the bulk silicate earth. Orogenic lamproites, including Mediterranean ones, are aligned towards high $^{87}Sr/^{86}Sr$ and low $^{143}Nd/^{144}Nd$ values, consistent with the involvement of a recycled crustal component with time-integrated high Rb/Sr and low Sm/Nd in the metasomatic agents of their mantle source. Anorogenic lamproites lie instead on a steeper trend towards unradiogenic $^{143}Nd/^{144}Nd$ values and low $^{87}Sr/^{86}Sr$ (Fig. 5a). Among Mediterranean lamproites a general geographic gradient can also be observed (Fig. 6): eastern Mediterranean lamproites (i.e. Balkan and Anatolian) show relatively lower $^{87}Sr/^{86}Sr$ and higher $^{143}Nd/^{144}Nd$ values, respectively, than western Mediterranean ones. Among the western Mediterranean lamproites we observe a progressive westward increase of radiogenic $^{87}Sr/^{86}Sr$ and unradiogenic $^{143}Nd/^{144}Nd$ from Italy and Spain (Fig. 6).

Pb isotopes composition of the Mediterranean lamproites (Fig. 5b, c) show high $^{207}Pb/^{204}Pb$ over $^{206}Pb/^{204}Pb$ with respect to the Northern Hemisphere Reference Line (NHRL, Hart 1984), confirming the ubiquitous, although variable, contribution of crustal components recycled in their mantle source.

The data broadly align along a trend starting from the composition of the GLOSS (Plank and Langmuir 1998) towards higher $^{207}Pb/^{204}Pb$ values. The same general array is observed in Figure 5c ($^{208}Pb/^{206}Pb$

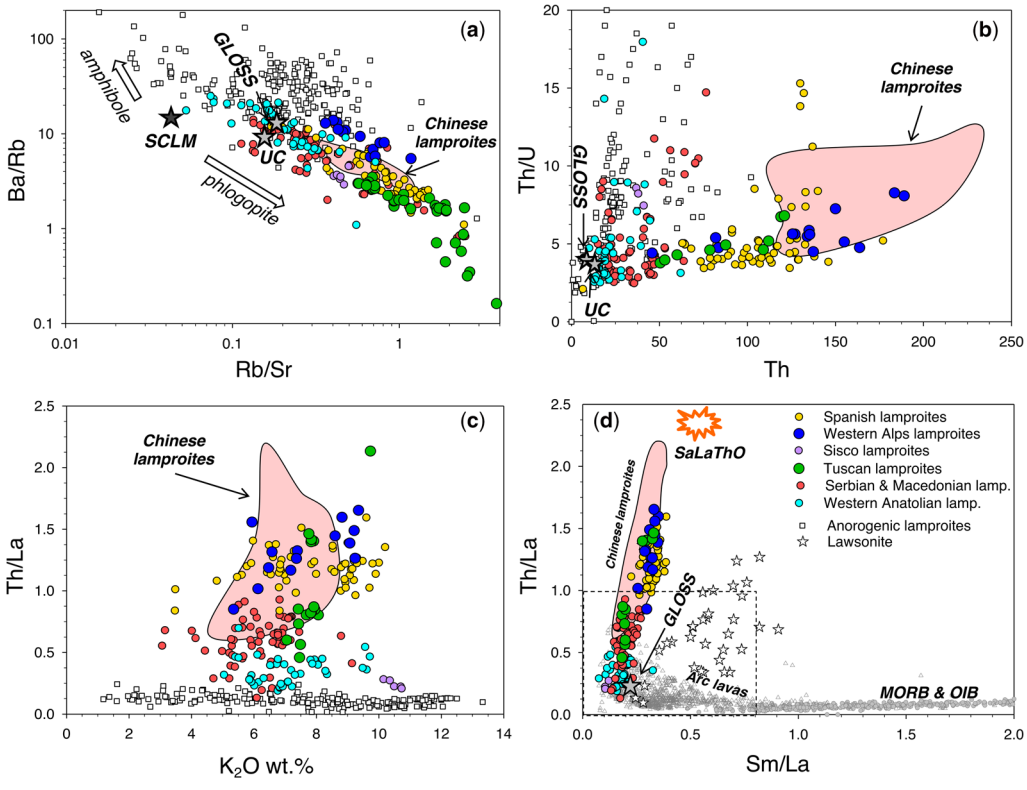

Fig. 4. Incompatible trace element ratios of orogenic and anorogenic lamproites. (**a**) Rb/Sr v. Ba/Rb (log scale); the arrows indicate the major role of phlogopite and amphibole respectively in the mantle source of orogenic and anorogenic lamproites. (**b**) Th/U v. Th highlighting the significant enrichment of Th. (**c**) Th/La v. K_2O showing the absence of correlation between the Th/La and the potassic character. (**d**) Th/La v. Sm/La of orogenic lamproites along with that of GLOSS (Plank and Langmuir 1998); arc magmas (Plank 2005); mid-ocean orogenic belt (MORB) (Gale *et al.* 2013) and ocean island basalt (OIB) (Willbold and Stracke 2006); the composition of published lawsonites (Martin *et al.* 2014; Wang *et al.* 2017) is also reported as stars. The dashed line encompasses the range reported in Figure 7. Data source as in Figure 2 (Table S1). Subcontinental Lithospheric Mantle (SCLM) from McDonough 1990; Upper Crust (UC) from Rudnick and Gao 2003; GLOSS from Plank and Langmuir 1998. Chinese lamproites are reported for comparison in a shaded field (Miller *et al.* 1999; Gao *et al.* 2007). Anorogenic lamproites are shown with a unique symbol and include ultrapotassic rocks from Australia (McCulloch *et al.* 1983; Jaques *et al.* 1986; Nelson *et al.* 1986; Fraser *et al.* 1985; Jaques and Foley 2018), Antarctica (Murphy *et al.* 2002), USA (Vollmer *et al.* 1984; Fraser *et al.* 1985; Lambert *et al.* 1995; Mirnejad and Bell 2006; Badal *et al.* 2014) and Russia (Davies *et al.* 2006).

v. $^{206}Pb/^{204}Pb$) where the investigated rocks display again a general array that departs from the GLOSS and deviates from the NHRL towards higher $^{208}Pb/^{206}Pb$ at low $^{206}Pb/^{204}Pb$ (Fig. 5c). Overall, the Pb isotope composition of Mediterranean lamproites is well distinct from that of anorogenic ones, which plot at significantly less radiogenic values of $^{206}Pb/^{204}Pb$ (Murphy *et al.* 2002; Mirnejad and Bell 2006; Jaques and Foley 2018).

Discussion

Orogenic lamproites represent exotic and rare mantle-derived magmas believed to originate in highly metasomatized lithospheric mantle domains (Peccerillo *et al.* 1988; Conticelli *et al.* 1992, 2002, 2007, 2015; Prelević *et al.* 2005, 2008, 2010; Prelević and Foley 2007).

High $^{87}Sr/^{86}Sr$ and low $^{143}Nd/^{144}Nd$ isotopic values of mantle-derived basaltic rocks are classically interpreted as due to shallow level crustal contamination. In the case of orogenic lamproites, however, a major role for crustal contamination is excluded by several evidences (Conticelli 1998; Murphy *et al.* 2002; Prelević *et al.* 2004, 2005; Conticelli *et al.* 2007, 2015), such as: (1) high MgO and compatible elements contents, such as Co, Ni and Cr, which are not derived from olivine cumulation; (2)

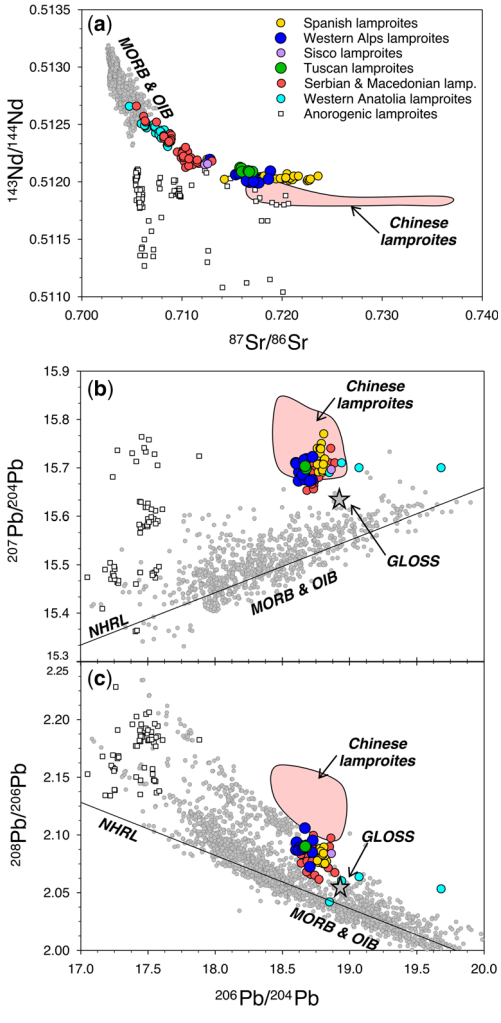

Fig. 5. Radiogenic Sr–Nd–Pb isotope composition of orogenic and anorogenic lamproites. (**a**) $^{87}Sr/^{86}Sr$ v. $^{143}Nd/^{144}Nd$; (**b**) $^{206}Pb/^{204}Pb$ v. $^{207}Pb/^{204}Pb$; (**c**) $^{206}Pb/^{204}Pb$ v. $^{208}Pb/^{206}Pb$. Data source as in Figures 2 and 4 (Table S1). Northern Hemisphere Reference Line (NHRL, Hart 1984), MORB and OIB (Stracke *et al.* 2003).

the presence of mafic mineral phases (e.g. high Fo-olivine and clinopyroxene) in equilibrium with their bulk compositions (Conticelli *et al.* 1992, 2007, 2015; Prelević and Foley 2007; Ammannati *et al.* 2016), excluding both cumulus and crustal contamination processes; (3) incompatible trace element contents significantly higher than continental crust composition (e.g. Rudnick and Gao 2003 and references therein). Therefore, the exotic isotopic and geochemical characteristics of Mediterranean lamproites must be related to processes directly affecting their mantle sources.

Combining mineral chemistry data with bulk rock major and trace elements and Sr–Nd–Pb isotopes previous studies have identified at least three different mantle components (Prelević *et al.* 2005; Conticelli *et al.* 2009; Tommasini *et al.* 2011).

An original ultra-depleted mantle source, with unradiogenic Pb and Sr isotopes and high $^{143}Nd/^{144}Nd$, is indicated by the low CaO and Al_2O_3 contents of all Mediterranean Lamproites and by the presence of high Fo-olivine with Cr-rich spinel inclusions (e.g. Arai 1994; Conticelli *et al.* 2015 and references therein).

A K-rich component re-fertilizing the depleted mantle source is required to impart the extreme incompatible trace element enrichment along with the crust-like Sr and Nd isotope signature. This metasomatic component is believed to derive from subduction-related sediment melts that permeated and reacted with the depleted peridotitic mantle, producing a orthopyroxene/phlogopite-rich (Fig. 4a) vein network (Foley 1992; Conticelli *et al.* 2015; Prelević and Foley 2007; Ammannati *et al.* 2016).

The high Th/La and Sm/La values of many Mediterranean lamproites require the further involvement of the above-mentioned SALATHO component (Tommasini *et al.* 2011) (Fig. 4d). This particular characteristic is not correlated with the K-enrichment (Fig. 4c) and thus not reconcilable with typical subduction-related processes such as the sediment recycling described above.

The evidence for the SALATHO component is not unique to Mediterranean lamproites but represents a specific characteristic of all the orogenic Tethyan Realm Lamproites, recurring also more than 10 000 km to the East in Tibet (Tommasini *et al.* 2011). Among Mediterranean lamproites, those from Spane and Italy display a more marked SALATHO signature, whilst those from other localities such as Corsica, Serbia and Western Anatolia show lower evidence of this component (Fig. 4d), which is likely overprinted by a larger contribution from the more 'typical' sediment melt (Prelević *et al.* 2005; Tommasini *et al.* 2011).

Possible origins for the SALATHO component

As seen above, the SALATHO component represents a specific characteristic of all Tethyan Realm Lamproites which is difficult to explain with the processes typically characterizing subduction-related magmatism (Tommasini *et al.* 2011). The budget of incompatible trace elements in subduction zones and in the related magmatism is largely controlled by the solubility of accessory phases during sediment melting, which also depends on the subducted lithology, that are able to concentrate and selectively

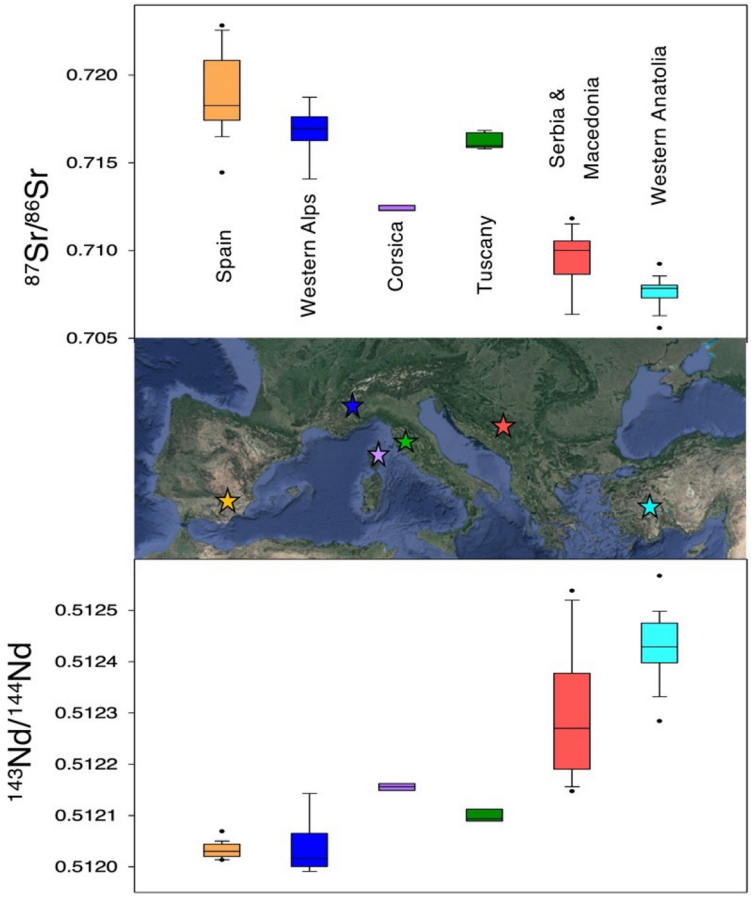

Fig. 6. Geographic variation of Sr and Nd isotope ratios in Mediterranean lamproites. Data source as in Figure 2 (Table S1). The boxes include the median value and are delimited by the 25th and the 75th percentiles of each population; the whiskers show the tenth and the 90th percentiles, whilst the dots represent the outliers at the fifth and 95th percentiles.

release specific elements (Klimm *et al.* 2008; Hermann and Rubatto 2009; Skora and Blundy 2010; Martindale *et al.* 2013; Skora *et al.* 2015; Avanzinelli *et al.* 2009, 2012, 2018; Casalini *et al.* 2019). In particular, Th and REEs are likely controlled by the possible presence of residual apatite, allanite or monazite (Klimm *et al.* 2008; Avanzinelli *et al.* 2009, 2012; Hermann and Rubatto 2009; Skora and Blundy 2010; Martindale *et al.* 2013) during partial melting of subducted sediments, whilst Nb and other HFSEs seems to be controlled by the solubility of rutile (e.g. Klimm *et al.* 2008). During subduction, at the temperature and pressure conditions able to induce partial melting of the sediments, the solubility of the accessory allanite/monazite increases significantly up to reaching the condition of complete removal from the residue, resulting in a massive release of Th, U and REE into the melt. On the other hand, experimental studies demonstrate that rutile remains oversaturated (i.e. residual; Kessel *et al.* 2005; Klimm *et al.* 2008; Hermann and Rubatto 2009), hence retaining Nb, Ta and Ti.

The presence/absence of such accessory phases during sediment melting exerts a strong control on the composition of sediment-dominated, subduction-related magmas, in particular dictating their variable Th/U (Avanzinelli *et al.* 2009, 2012) and determining their ubiquitous depletion in Nb and Ta (Klimm *et al.* 2008; Avanzinelli *et al.* 2009, 2012). In this context, the role of possible accessory phases can be considered also to explain the exotic SALATHO component.

Recently, Soder and Romer (2018) working on Variscan lamprophyres from southwestern Germany and eastern France, which share similar Th/La and Sm/La to Mediterranean lamproites, attributed the

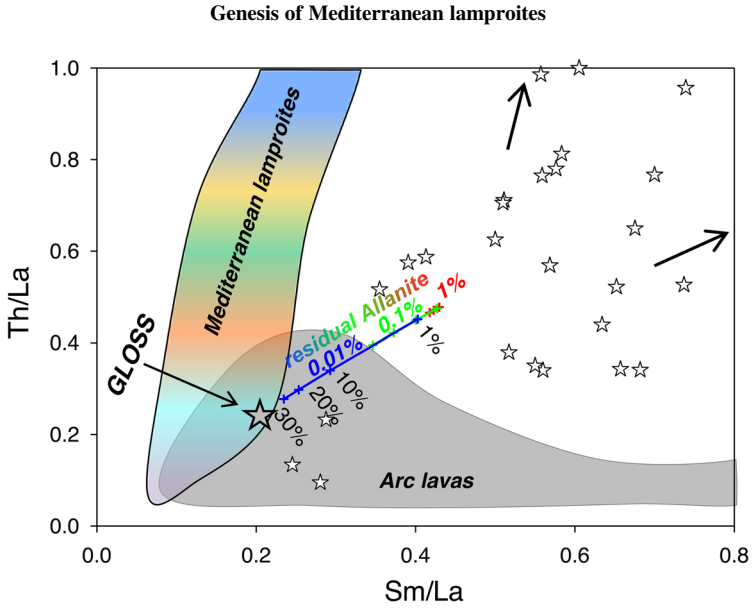

Fig. 7. Th/La v. Sm/La plot showing the calculated composition of partial melts (F = 1–30%) of a GLOSS-like subducting sediment with variable amount of residual allanite (1, 0.1 and 0.01%). The modelled ratios remain below those of lamproites and of lawsonite (Fig. 4d, Martin *et al.* 2014; Wang *et al.* 2017). Consider that the whole range of lawsonite composition extends over the plot, up to Sm/La = 0.9 and Th/ La = 4.8 (Martin *et al.* 2014) as shown by the arrows.

genesis of the SALATHO component to residual allanite during partial melting of subducted sediments metasomatizing the sub-continental lithospheric mantle, and subsequent melting of the metasomatized mantle domains during post-collisional lithospheric extension. We have tried to model this hypothesis using the partition coefficients of allanite (Klimm *et al.* 2008), the composition of GLOSS (Plank and Langmuir 1998) and assuming different percentages of residual allanite (1, 0.1 and 0.01%) along with different degrees of partial melting ($F = 1$–30%) (Fig. 7). The results clearly show that residual allanite, owing to its $D^{La} > D^{Th} \geq D^{Sm}$, is liable to create a metasomatizing melt with roughly twice Th/La and Sm/La of the starting GLOSS source, but the values remain well below those observed in lamproites (Fig. 7). Also, in our model we have assumed that the budget of Th, La and Sm is controlled only by allanite, and this cannot be the case given that melts from subducted sediments show a general slight increase in Th/La and decrease in Sm/La with respect to their sources (Johnson and Plank 1999; Hermann and Rubatto 2009; Skora and Blundy 2010; Wang *et al.* 2017). In any case, allanite-saturated sediment melts are expected to have low Th/U, which is the opposite of what is observed in orogenic lamproites that are always characterized by extremely high Th/U (Fig. 4b).

The alternative model, originally postulated by Tommasini *et al.* (2011) and successively confirmed by other studies (Lustrino *et al.* 2016; Wang *et al.* 2017, 2019; Wang and Foley 2020), involves the participation of lawsonite-bearing low-grade metamorphic rocks in controlling this peculiar feature of orogenic lamproites. Indeed, lawsonite is a major repository for Sr, Pb, U, Th and LREEs (Spandler *et al.* 2003; Usui *et al.* 2006; Martin *et al.* 2014), and a number of Th, La, Sm compositions of lawsonite (Martin *et al.* 2014; Vitale Brovarone *et al.* 2014; Wang *et al.* 2017) are reported in Figure 7. These lawsonites clearly have high Th/La and Sm/La, the latter even higher than that recorded in Mediterranean lamproites, and upon melting (Tommasini *et al.* 2011) or dehydration (Lustrino *et al.* 2016) are capable of imparting to lamproite magmas their unique trace element signature (see below). In the case of melting, in order to produce the high Th/La and Sm/La, lawsonite must have been totally consumed. The recent experimental work of Wang and Foley (2020), specifically designed to investigate the role of blue schists stored in the shallow lithosphere (2GPa), showed that upon melting lawsonite is completely removed from the residue at 800°C, producing melts enriched in Th/La with respect to their lawsonite-rich crustal protoliths.

Tommasini *et al.* (2011) suggested that the SALATHO signature can be ascribed to the stabilization and long-term (*c.* 300–500 Myr, see fig. 8 in Tommasini *et al.* 2011) storage of lawsonite linked to chaotic mélanges of subducted altered oceanic

crust (basalt and sediments) at relatively low grade of metamorphism. This is indicated by the high $^{208}Pb/^{206}Pb$ values over $^{206}Pb/^{204}Pb$ (Fig. 5b) of orogenic lamproites, requiring high time-integrated ($^{232}Th/^{238}U$) and relatively low time-integrated ($^{238}U/^{204}Pb$). These mélange domains experienced different storage times in each sector of the Tethyan Realm orogenic belts, in agreement with the diachronous collision of the northward drifting continental slivers from Gondwana (e.g. Hun Terrane, Variscan and Cimmerian terranes; Stampfli 2000; Stampfli and Borel 2002; Gaetani *et al.* 2003; Scotese 2004). Incidentally, the occurrence of the SALATHO component has been observed in the so-called lampyrites outcropping in the Variscan Bohemian Massif (Krmíček *et al.* 2020), and provides further support for a long storage time of these mélange domains within the subcontinental lithospheric mantle.

The lithospheric mantle source of Mediterranean Lamproites

It is widely accepted that a normal four-phase peridotitic mantle cannot represent the source of lamproitic magmas, which requires the presence of an additional K-rich hydrous mineral, generally identified as phlogopite (Mitchell and Bergman 1991; Foley 1992, 1993). Accordingly, previous studies interpreted lamproitic magmas as the products of partial melting of metasomatized sub-continental refractory lithospheric mantle (e.g. Foley *et al.* 1987; Foley and Venturelli 1989; Conticelli 1998; Prelević and Foley 2007). Since the pioneering work of Foley (1992), it was suggested that large volumes of metasomatic components, required to generate the peculiar geochemical and isotopic characteristics of the mantle source of lamproite magmas, are accommodated within a vein network in the sub-continental lithospheric mantle (Foley 1992; Conticelli *et al.* 2002, 2007, 2009; 2015; Prelević and Foley 2007; Prelević *et al.* 2008; Avanzinelli *et al.* 2009, 2020; Ammannati *et al.* 2016; Dallai *et al.* 2019). It was experimentally demonstrated that K-rich metasomatizing agents may react with the depleted peridotitic mantle producing phlogopite-rich veins (Sekine and Wyllie 1982; Foley 1990, 1992; Conceição and Green 2004). Other studies, mainly based on the high Ni content of high-Fo olivine crystals, have indicated that subduction-derived silica-rich melts would react with the peridotitic mantle producing orthopyroxene at the expense of olivine (Straub *et al.* 2008; Foley *et al.* 2013). Within a pyroxenitic assemblage without olivine (high D^{Ni}), Ni will be mostly hosted in pyroxene (lower D^{Ni}), resulting, after partial melting, in magmas with higher Ni contents, hence later crystallizing high-Ni olivine phenocrysts (Straub *et al.* 2008; Foley *et al.* 2013). The recent study of Ammannati *et al.* (2016) showed extremely high Ni in high-Fo olivine in Italian orogenic lamproites, confirming the key role of orthopyroxene-rich domains (i.e. veins) in the mantle source of these magmas. Therefore, the presence of phlogopite–orthopyroxene domains in the lithospheric mantle seems to be required to generate lamproite-like magmas. Natural evidence of subduction-related, orthopyroxene-generating metasomatic agents, sometimes associated with the presence of phlogopite, have been observed in ultramafic xenoliths from several localities affected by orogenic metasomatism (Brandon *et al.* 1999; Grégoire *et al.* 2001; Franz *et al.* 2002), also in the Mediterranean area and surroundings (Cvetković *et al.* 2004*b*; Kovács *et al.* 2007), as well as in the Finero peridotite massif (Zanetti *et al.* 1999).

A particularly intriguing case is provided by the mantle xenoliths erupted within the Na-alkaline anorogenic volcanism of Tallante, which post-dates the ultrapotassic magmatism with lamproitic affinity of Murcia in southeastern Spain (e.g. Duggen *et al.* 2005). These mantle xenoliths display extreme compositional and mineralogical heterogeneities (Arai *et al.* 2003; Beccaluva *et al.* 2004; Shimizu *et al.* 2005; Rampone *et al.* 2010; Bianchini *et al.* 2011, 2015; Martelli *et al.* 2011; Bianchini and Natali 2017; Marchesi *et al.* 2017; Dallai *et al.* 2019; Avanzinelli *et al.* 2020). Many of them are anhydrous lherzolite to harzburgite reflecting mantle depletion and impregnation with various melt in anorogenic conditions (Beccaluva *et al.* 2004; Rampone *et al.* 2010; Bianchini *et al.* 2011). Other xenoliths show clear evidence of metasomatism resulting in neoformation of orthopyroxene, plagioclase, phlogopite and pargasitic amphibole, indicating a lithospheric mantle modified by hydrous, subduction-related metasomatic agents (Arai *et al.* 2003; Beccaluva *et al.* 2004).

Among this large xenolith variability, the Tallante magmas also exhumed rare composite xenoliths where peridotite is locally crosscut by felsic veins containing plagioclase and orthopyroxene ± quartz ± phlogopite ± amphibole (Arai *et al.* 2003; Beccaluva *et al.* 2004; Shimizu *et al.* 2005; Bianchini *et al.* 2011; Dallai *et al.* 2019; Avanzinelli *et al.* 2020). These mineralogical associations are again consistent with the postulated lithospheric mantle source of lamproitic magmas, characterized by the reaction of the depleted mantle with crustal-derived, hydrous, silica-oversaturated melts rich in alkalis. Within the composite xenoliths of Tallante, Avanzinelli *et al.* (2020) also documented the presence of a millimetric veinlet hosting accessory minerals such as apatite, thorite/huttonite, rutile and graphite, hence producing isolated domains particularly enriched in incompatible trace elements. Overall, the compositional variability of mantle xenoliths

erupted at Tallante testifies the presence, in a region where lamproites were produced, of an extremely heterogeneous mantle, characterized by a number of metasomatic events producing different domains, which upon melting may be capable of generating lamproites, hence providing an extraordinary window on the possible mantle sources of these extremely peculiar magmas.

The detailed study by Avanzinelli *et al.* (2020) on veined mantle xenoliths from Tallante, reported some key features that may confirm the link between these xenoliths and lamproites, especially regarding the occurrence of the SALATHO component within the metasomatized lithospheric mantle. Their data showed that the effect of metasomatism is not confined to the mineral phases of the felsic vein and the orthopyroxene-rich reaction zone (i.e. in plagioclase and orthopyroxene), but it permeated also the surrounding peridotitic mantle, as also observed in peridotite Massifs (Woodland *et al.* 1996). Indeed, the clinopyroxene (and orthopyroxene) of the peridotitic portion of the Tallante veined xenolith, which had not experienced any mineralogical modification, preserve geochemical and isotopic evidence of the metasomatic enrichment. They show anomalous incompatible trace element and 'm-shaped' REE pattern (Avanzinelli *et al.* 2020), being extremely enriched in middle (M)REE and Th, but depleted in LREE. The origin of such a peculiar composition has to be related to the geochemical characteristic of the metasomatic melts (see previous section) and/or in the competing role of the other phases equilibrating in the same portion of the mantle (Avanzinelli *et al.* 2020). In any case, upon partial melting such anomalous pyroxene would produce melts enriched with Th and Sm over La, hence imparting the characteristic SALATHO flavour common to all Tethyan Realm Lamproites.

In order to better define the origin of SALATHO, we calculated the hypothetic incompatible trace element composition (Fig. 8) of partial melts in equilibrium with clinopyroxene, orthopyroxene and plagioclase hosted in the various portions of the veined xenoliths (i.e. surrounding mantle, vein envelope, vein) reported in Avanzinelli *et al.* (2020) using a selected set of partition coefficients (Green *et al.* 2000; Foley and Jenner 2004; Aigner-Torres *et al.* 2007; Fig. 8). It is worth emphasizing that using different sets of partition coefficients the results shown in Figure 8 do not change significantly.

Figure 8 shows that melts in equilibrium with clino- and orthopyroxenes have invariably high Th/La and Sm/La reaching values (up to 10.4 and 3.6, respectively, in clinopyroxene Fig. 8a), as well as extreme enrichment in Th (up to almost 300 ppm, Fig. 8b). Melts in equilibrium with plagioclase show lower Th content and Th/La ratios, and variable but still relatively high Sm/La (up to 0.87). A bulk composition of the partial melts deriving from such a veined mantle is extremely difficult to model. This would require assumptions on the exact knowledge of the relative proportions between the vein, the reaction zone and the surrounding peridotite involved in the melting process. In addition, lamproitic magmas are likely made up by the sum of several different melts deriving various portions of the metasomatized mantle (see previous section). For example, a significant contribution to the composition of Mediterranean lamproites must derive from melting of phlogopite-rich mantle domains (see previous discussion; Conticelli *et al.* 2015; Ammannati *et al.* 2016). The modelled melts in equilibrium with each single mineral (clinopyroxene, orthopyroxene and plagioclase; Fig. 8), however, clearly show that even a small amount of such melts may impart the characteristic high Th/La and Sm/La to the erupted lamproites. In such, the described mantle xenoliths likely represent the portion of the lithospheric mantle hosting the SALATHO component required by orogenic lamproites.

Further considerations can be done on the basis of isotopic composition. The Pb isotope composition of the aforementioned xenoliths is similar to that of Spanish lamproites, with high $^{208}Pb/^{206}Pb$ over $^{206}Pb/^{204}Pb$ (see Fig. 5b). The comparison for Sr and Nd isotope ratios is not as good, although they could be dominated by melts deriving from phlogopite-rich domains with higher $^{87}Sr/^{86}Sr$ and lower $^{143}Nd/^{144}Nd$. The high $^{208}Pb/^{206}Pb$ is also consistent with a high time integrated (*c.* 300–500 Myr) Th/U of the metasomatic melts (Tommasini *et al.* 2011). This long-term storage, however, seems to be related to the crustal component from which the melts were generated rather than to the age of the metasomatic processes, which instead appears to be rather recent. Dallai *et al.* (2019) measured oxygen isotopes in the same veined samples described above, reporting continuously decreasing $\delta^{18}O$ values, from the vein, which had typically crustal values (up to 10.5), to typical mantle values in the surrounding peridotite. The authors calculated that, in order to preserve such a difference from diffusion-assisted re-equilibration, the metasomatic process (i.e. the vein formation) must have occurred <5 Myr before their entrapment in the Tallante magmas. The same is supported by the large variability in Sr isotope in the same sample, from the vein (0.7124) to the peridotite (0.7060) (Avanzinelli *et al.* 2020).

Petrogenesis of Mediterranean lamproites and geodynamic relationships

Based on the available evidence described above we suggest that Mediterranean lamproites were generated during the late stage of plate convergence

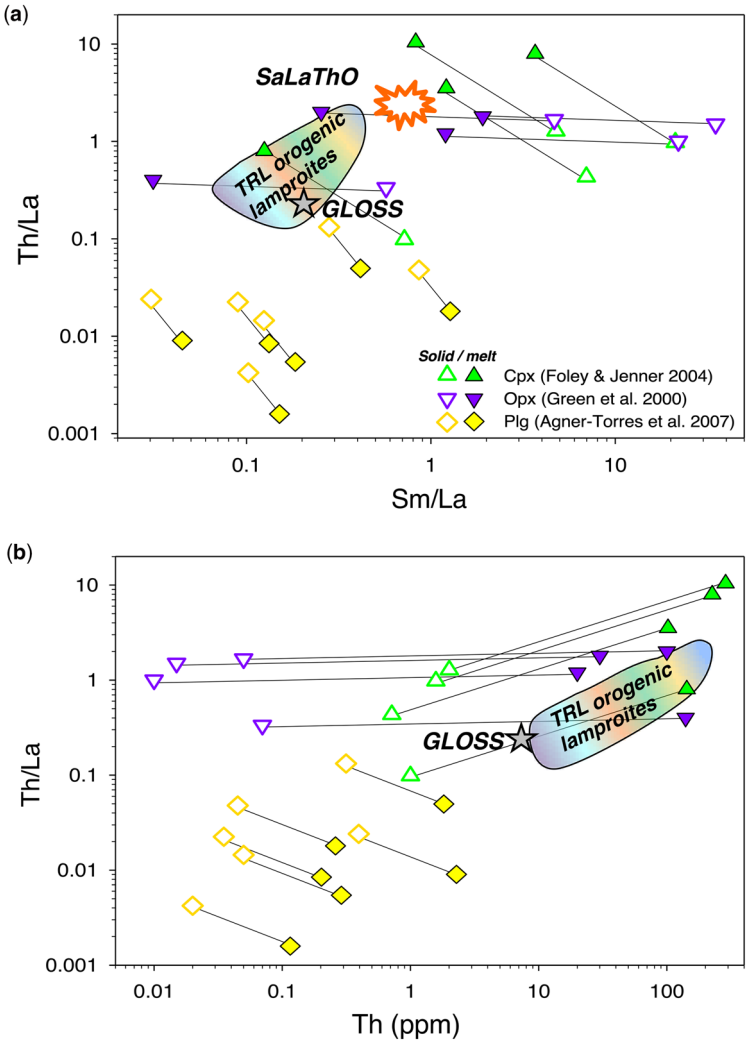

Fig. 8. (**a**) Th/La v. Sm/La and (**b**) Th/La v. Th (log scale) of clinopyroxene (Cpx), orthopyroxene (Opx) and plagioclase (Plg) (open symbols) from Tallante xenoliths (Avanzinelli *et al.* 2020) and melts in equilibrium with them (solid symbols). Partition coefficients calculated on lamproite rocks were used where available (i.e. Cpx). The partition coefficients used for the calculations are (1) Cpx, $D^{La} = 0.057$, $D^{Sm} = 0.328$, $D^{Th} = 0.007$ (Foley and Jenner 2004); (2) Opx, $D^{La} = 0.006$, $D^{Sm} = 0.011$, $D^{Th} = 0.0005$ (Green *et al.* 2000); (3) Plg, $D^{La} = 0.065$, $D^{Sm} = 0.044$, $D^{Th} = 0.173$ (Aigner-Torres *et al.* 2007)); partition coefficients for Cpx were calculated directly on lamproitic rocks. TRL, Tethyan Realm Lamproites.

characterized by continental collision and interlayering of mantle and continental slivers including low solidus crustal lithologies of different origins (Fig. 9). Similar crust-mantle mélanges are observed in massifs such as Ronda and Beni Bousera, where the exhumed fossil crust mantle boundary is characterized by mylonites and mélanges (Tubía *et al.* 2004; Platt *et al.* 2003, 2013; Bartoli *et al.* 2015). Similar cases of interlayered crust–mantle associations are common throughout and nearby the Mediterranean region, such as in the fossil deep crust–mantle sections of the Ivrea-Verbano (Quick *et al.* 1995), the Ulten Zone (Braga and Massonne 2012) and central Calabria (Rizzo *et al.* 2001).

Lawsonite-rich crustal domains at high Th/La and Th/U hosted within the mélanges should have formed during an old events related to the diachronous collision of the northward drifting continental slivers from Gondwana in order to develop their high $^{208}Pb/^{206}Pb$ (Tommasini *et al.* 2011).

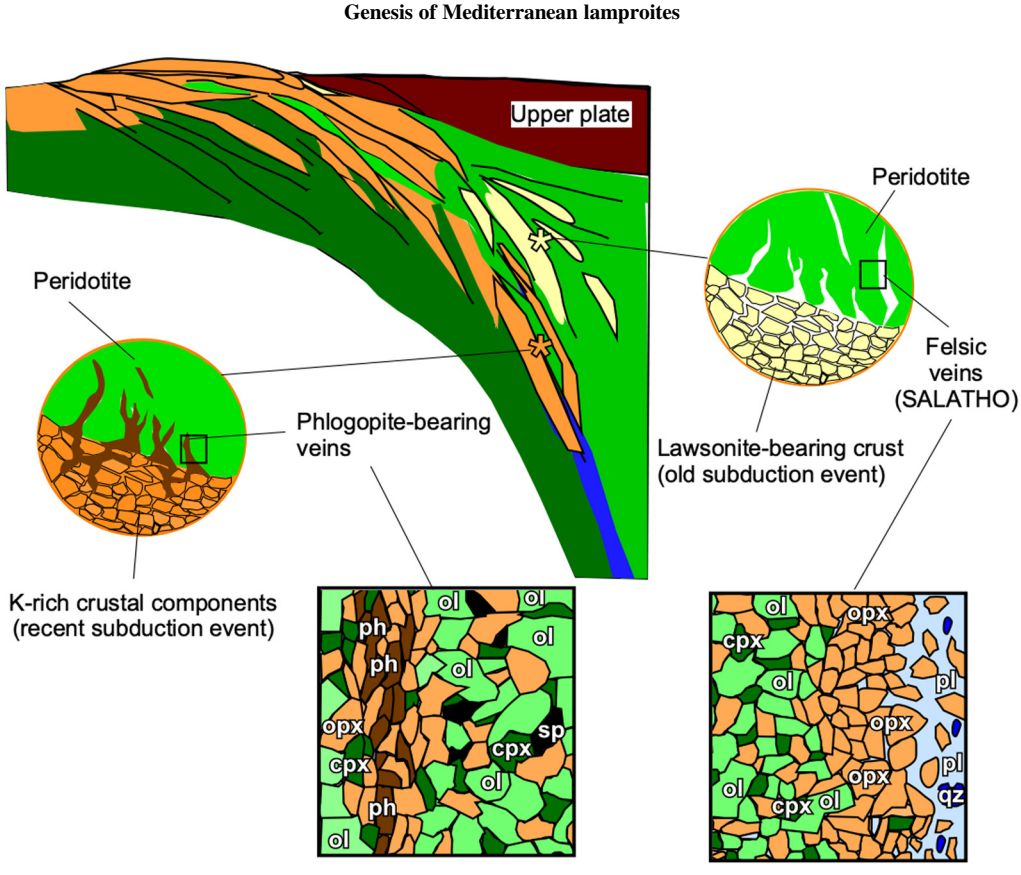

Fig. 9. Suggested schematic scenario for the genesis of Mediterranean orogenic lamproites. Subducted crustal material of different ages is represented with different colours (light yellow, lawsonite-bearing crust from old subduction event; orange, K-rich crust from recent subduction event). Round insets show the development of the two sets of metasomatic veins (i.e. SALATHO-like and phlogopite bearing) responsible for the key geochemical and isotopic features of the studied magmas. The bottom squares provide cartoons of the metasomatic reactions and mineralogy of the modified mantle. The image of the felsic SALATHO-like vein reproduces the petrography of the Tallante composite mantle xenoliths (Avanzinelli *et al.* 2020), whilst that of the phlogopite-rich veins is based on the study of Ammannati *et al.* (2016).

The most recent subduction events (e.g. the Neo-Tethys and Alpine Tethys oceanic basin) and continental collision (Alpine, Apennine, Himalayan Orogeny), brought to depth further crustal material, which underwent partial melting and metasomatized the depleted lithospheric mantle domains of the previously accreted chaotic mélange. These melts imparted the K-rich flavour and subduction signature to the lithospheric mantle, likely as phlogopite–orthopyroxene vein network (Fig. 9; Foley 1992; Melzer and Foley 2000; Ammannati *et al.* 2016).

Successively, lithosphere extension, thermal relaxation and associated mantle uplift produced during back-arc extension (Platt *et al.* 2003, 2013), determined melting of the older lawsonite-rich crustal domains, completely exhausting lawsonite at relatively low temperature (i.e. 800°C; Wang and Foley 2020). These highly reactive SALATHO-like crustal melts segregated from their sources and reacted with the surrounding mantle domains, forming the felsic-veined mantle domains observed in the Tallante xenoliths (Dallai *et al.* 2019; Avanzinelli *et al.* 2020). Indeed, as indicated by oxygen isotopes, the formation of the felsic veins must have occurred relatively recently to prevent diffusion-assisted re-equilibration.

Proceeding with lithosphere extension and thermal relaxation, partial melting of such a heterogeneous and variable metasomatized mantle occurred, first affecting the different metasomatic veins (i.e. both phlogopite-rich and SALATHO-like), characterized by low solidus temperatures and continued progressively involving also the surrounding ambient peridotite. In this context, the geochemical and

isotopic variability of Mediteranean lamproites (and Tethyan lamproites in general) (Figs 4, 5 & 6) can be interpreted as the result of mixing of different batches of melt deriving from the various mantle domains. This process may also account for progressive dilution of the 'lamproitic' character in the less potassic members (Figs 2 & 3) (Avanzinelli *et al.* 2009; Conticelli *et al.* 2009; Mattei *et al.* 2014), along the lines of the vein-plus-wall rock melting mechanism (Foley 1992). Since the geochemical and isotopic crustal signature is not limited to the veins but permeates also the surrounding peridotite, melts deriving from different proportion of the various veins and surrounding peridotite will inherit variable levels of trace element and isotopic enrichment. Yet, some general common characteristics (e.g. high LILE/HFSE, high Th/La and Sm/La) are preserved also in higher degree melts producing the shoshonitic and calc-alkaline products.

In the proposed scenario the origin of Mediterranean lamproites occurs at rather shallow depths, likely within the spinel stability field. The mantle xenoliths erupted at Tallante, here suggested as representative of possible sources for the SALATHO component, are equilibrated at pressure (0.7–0.9 GPa; Rampone *et al.* 2010; Bianchini *et al.* 2011 and references therein) straddling the transition between plagioclase and spinel. Tuscan lamproites (Torre Alfina) erupted mantle xenoliths confined within the spinel stability field (1.5–2.2 GPa: Conticelli and Peccerillo 1990), suggesting slightly higher depths, yet never crossing the spinel garnet transition. Similar pressure ranges (0.7–2 GPa) are indicated by thermobarometric constraints based on phlogopite composition of Mediterranean lamproites (Fritschle *et al.* 2013). This is also consistent with the high silica contents of these magmas, despite their primitive composition.

The inferred shallow origin of orogenic Mediterranean lamproites represents a further distinctive characteristic that differentiate them from lamproites erupted in anorogenic settings. Anorogenic lamproites are indeed interpreted as originated at high depth (>4 GPa; Foley 1993, Edgar and Mitchell 1997, Mirnejad and Bell 2006; Jaques and Foley 2018) as also indicated by the occasional presence of diamond (McCulloch *et al.* 1983; Jaques *et al.* 1990; Lambert *et al.* 1995; Davies *et al.* 2006).

We conclude that orogenic lamproites, such as those of the Mediterranean and the Tethyan Realm in general, are rocks that characterize areas that were affected by multiple Wilson cycles, as observed in the Alpine–Himalayan Realm. They are originated at relatively shallow depth in a peridotite lithospheric mantle crosscut by several vein networks with different age and composition, but similar subduction-related origin. Late partial melting events mix variable contributions from the veins and the host peridotite, generating the observed spectrum of orogenic magmas that appears typical of the specific geodynamic framework.

Acknowledgements The authors would like to thank Stephen Foley and Michel Grégoire for their constructive and thorough criticisms.

Conflict of interest

The authors declare no known conflicts of interest associated with this publication.

Author contributions **MC**: conceptualization (equal), data curation (equal), investigation (equal), writing – original draft (equal), writing – review & editing (equal); **RA**: conceptualization (equal), data curation (equal), investigation (equal), supervision (equal), writing – original draft (equal), writing – review & editing (equal); **ST**: conceptualization (equal), investigation (equal), writing – original draft (equal), writing – review & editing (supporting); **CN**: data curation (supporting), investigation (equal), writing – original draft (supporting), writing – review & editing (supporting); **GB**: conceptualization (equal), writing – original draft (supporting), writing – review & editing (supporting); **DP**: conceptualization (equal), writing – original draft (supporting), writing – review & editing (supporting); **MM**: conceptualization (equal), writing – original draft (equal), writing – review & editing (equal); **SC**: conceptualization (equal), data curation (equal), funding acquisition (lead), investigation (equal), supervision (equal), validation (equal), writing – original draft (equal), writing – review & editing (equal).

Funding Financial support was provided by the Università degli Studi di Firenze (DST – ex. 60% funds) issued to Martina Casalini, by the Italian Ministry of Education and Research (MIUR) through PRIN_2015 (research grants #: 20158A9CBM and 2020BW8MY5).

Data availability All data generated or analysed during this study are included in this published article (and its supplementary information files).

References

Aigner-Torres, M., Blundy, J., Ulmer, P. and Pettke, T. 2007. Laser Ablation ICPMS study of trace element partitioning between plagioclase and basaltic melts: an experimental approach. *Contributions to Mineralogy and Petrology*, **153**, 647–667, https://doi.org/10.1007/s00410-006-0168-2

Akal, C. 2008. K-richterite-olivine-phlogopite-diopside-sanidine lamproites from the Afyon volcanic province, Turkey. *Geological Magazine*, **145**, 570–585, https://doi.org/10.1017/S0016756808004536

Allen, M.B. and Armstrong, H.A. 2008. Arabia-Eurasia collision and the forcing of mid-Cenozoic global

cooling. *Palaeogeography, Palaeoclimatology, Palaeoecology*, **265**, 52–58, https://doi.org/10.1016/j.palaeo.2008.04.021

Altherr, R., Meyer, H.P., Holl, A., Volker, F., Alibert, C., McCulloch, M.T. and Majer, V. 2004. Geochemical and Sr-Nd-Pb isotopic characteristics of Late Cenozoic leucite lamproites from the East European Alpine belt (Macedonia and Yugoslavia). *Contribution to Mineralogy and Petrology*, **147**, 58–73, https://doi.org/10.1007/s00410-003-0540-4

Ammannati, E., Jacob, D.E., Avanzinelli, R., Foley, S.F. and Conticelli, S. 2016. Low Ni olivine in silica-undersaturated ultrapotassic igneous rocks as evidence for carbonate metasomatism in the mantle. *Earth and Planetary Science Letters*, **444**, 64–74, https://doi.org/10.1016/j.epsl.2016.03.039

Arai, S. 1994. Compositional variation of olivine–chromian spinel in Mg-rich magmas as a guide to their residual spinel peridotites. *Journal of Volcanology and Geothermal Research*, **59**, 279–293, https://doi.org/10.1016/0377-0273(94)90083-3

Arai, S., Shimizu, Y. and Gervilla, F. 2003. Quartz diorite veins in a peridotite xenolith from Tallante, Spain: implications for reactions and survival of slab-derived SiO_2- oversaturated melts in the upper mantle. *Proceedings of the Japan Academy Series B*, **79**, 145–150, https://doi.org/10.2183/pjab.79B.141

Arculus, R.J. 2003. Use and abuse of the terms calcalkaline and calcalkalic. *Journal of Petrology*, **44**, 929–935, https://doi.org/10.1093/petrology/44.5.929

Avanzinelli, R., Lustrino, M., Mattei, M., Melluso, L. and Conticelli, S. 2009. Potassic and ultrapotassic magmatism in the circum-Tyrrhenian region: significance of carbonated pelitic v. pelitic sediment recycling at destructive plate margin. *Lithos*, **113**, 213–227, https://doi.org/10.1016/j.lithos.2009.03.029

Avanzinelli, R., Prytulak, J., Heumann, A., Koetsier, G. and Elliott, T. 2012. Combined ^{238}U–^{230}Th and ^{235}U–^{231}Pa constraints on the transport of slab-derived material beneath the Mariana Islands. *Geochimica et Cosmochimica Acta*, **92**, 308–328, https://doi.org/10.1016/j.gca.2012.06.020

Avanzinelli, R., Casalini, M., Elliott, T. and Conticelli, S. 2018. Carbon fluxes form subducted carbonates revealed by uranium excess at Mount Vesuvius, Italy. *Geology*, **46**, 259–262, https://doi.org/10.1130/G39766.1

Avanzinelli, R., Bianchini, G. *et al*. 2020. Subduction-related hybridization of the lithospheric mantle revealed by trace element and Sr-Nd-Pb isotopic data in composite xenoliths from Tallante (Betic Cordillera, Spain). *Lithos*, **352–353**, 105316, https://doi.org/10.1016/j.lithos.2019.105316

Badal, J., Carlson, R.W., Frost, C.D., Hearn, B.C., Jr and Eby, G.N. 2014. Continent-scale linearity of kimberlite-carbonatite magmatism, mid-continent North America. *Earth and Planetary Science Letters*, **403**, 1–14, https://doi.org/10.1016/j.epsl.2014.06.023

Barberi, F., Innocenti, F. and Ricci, C.A. 1971. La Toscana meridionale. Il magmatismo. *Rendiconti della Società Italiana di Mineralogia e Petrologia*, **27**, 169–210.

Barnekow, P. 2000. *Volcanic rocks from central Italy: an Oxygen isotopic microanalytical and geochemical study*. PhD thesis, University of Gottingen.

Barnekow, P., Hoefs, J. and Peccerillo, A. 1998. *In-situ* measurement of oxygen isotope ratios by laser ablation mass spectrometry – an example from the Torre Alfina volcano, Central Italy. *Mineralogical Magazine*, **62A**, 120–121, https://citeseerx.ist.psu.edu/viewdoc/download?doi=10.1.1.869.4251&rep=rep1&type=pdf

Bartoli, O., Acosta-Vigil, A. and Cesare, B. 2015. High-temperature metamorphism and crustal melting: working with melt inclusions. *Periodico di Mineralogia*, **84**, 591–614, https://doi.org/10.2451/2015PM0434

Beccaluva, L., Bianchini, G., Bonadiman, C., Siena, F. and Vaccaro, C. 2004. Coexisting anorogenic and subduction-related metasomatism in mantle xenoliths from the Betic Cordillera (southern Spain). *Lithos*, **75**, 67–87, https://doi.org/10.1016/j.lithos.2003.12.015

Benito, G.R., Lopez Ruiz, J., Cebria, J.M., Hertogen, J., Doblas, M., Oyarzun, R. and Demaiffe, D. 1999. Sr and O isotope constraints on source and crustal contamination in the High-K calc-alkaline and shoshonitic Neogene volcanic rocks of SE Spain. *Lithos*, **46**, 773–802, https://doi.org/10.1016/S0024-4937(99)00003-1

Bianchini, G. and Natali, C. 2017. Carbon elemental and isotopic composition inmantle xenoliths from Spain: insights on sources and petrogenetic processes. *Lithos*, **272–273**, 84–91, https://doi.org/10.1016/j.lithos.2016.11.020

Bianchini, G., Beccaluva, L., Nowell, G.M., Pearson, D.G. and Siena, F. 2011. Mantle xenoliths from Tallante (Betic Cordillera): insights into the multi-stage evolution of the south Iberian lithosphere. *Lithos*, **124**, 308–318, https://doi.org/10.1016/j.lithos.2010.12.004

Bianchini, G., Braga, R., Langone, A., Natali, C. and Tiepolo, M. 2015. Metasedimentary and igneous xenoliths from Tallante (Betic Cordillera, Spain): inferences on crust–mantle interactions and clues for post-collisional volcanism magma sources. *Lithos*, **220**, 191–199, https://doi.org/10.1016/j.lithos.2015.02.011

Borghetti, G., Sbrana, A. and Sollevanti, F. 1981. Vulcanotettonica dell'area dei Monti Cimini e rapporti cronologici tra vulcanismo Cimino e Vicano. *Rendiconti Società Geologica Italiana*, **4**, 253–254.

Borsi, S., Ferrara, G. and Tongiorgi, E. 1967. Determinazione con il metodo K/Ar delle età delle rocce magmatiche della Toscana. *Bollettino Società Geologica Italiana*, **86**, 403–410.

Bortolotti, V., Chiari, M., Marroni, M., Pandolfi, L., Principi, G. and Saccani, E. 2013. Geodynamic evolution of ophiolites from Albania and Greece (Dinaric-Hellenic belt): one, two, or more oceanic basins*? International Journal of Earth Sciences*, **102**, 783–811, https://doi.org/10.1007/s00531-012-0835-7

Braga, R. and Massonne, H.-J. 2012. H_2O content of deep-seated orogenic continental crust: the Ulten Zone, Italian Alps. *International Geology Review*, **54**, 633–641, https://doi.org/10.1080/00206814.2010.548155

Brandon, D.A., Becker, H., Carlson, R.W. and Shirey, S.B. 1999. Isotopic constraints on time scales and mechanisms of slab material transport in the mantle wedge: evidence from the Simcoe mantle xenoliths, Washington, USA. *Chemical Geology*, **160**, 387–407, https://doi.org/10.1016/S0009-2541(99)00109-6

Callegari, E., Cigolini, C., Medeot, O. and D'Antonio, M. 2004. Petrogenesis of Calc-alkaline and shoshonitic

post-collisional Oligocene volcanics of the Cover Series of the Sesia Zone, Western Italian Alps. *Geodinamia Acta*, **17**, 1–29, https://doi.org/10.3166/ga.17.1-29

Carraro, F. and Ferrara, G. 1978. Alpine tonalite at Miagliano, Biella (zone diorite-kinzigitica). *Schweizerische Mineralogische und Petrographische Mitteilungen*, **48**, 75–80, https://doi.org/0.5169/seals-37751

Casalini, M. 2018. $^{98}Mo/^{95}Mo$ and $^{238}U/^{235}U$ in lamproites, shoshonites, and high-K calc-alkaline rocks from Western Alps: inferences on their genesis. *Italian Journal of Geoscience*, **137**, 465–477, https://doi.org/10.3301/IJG.2018.20

Casalini, M., Avanzinelli, R., Tommasini, S., Elliott, T. and Conticelli, S. 2019. Ce/Mo and molybdenum isotope systematics in subduction-related orogenic potassic magmas of Central-Southern Italy. *Geochemistry, Geophysics, Geosystems*, **20**, 2753–2768, https://doi.org/10.1029/2019GC008193

Chelazzi,L., Bindi, L., Olmi, F., Peccerillo, A., Menchetti, S. and Conticelli, S. 2006. A lamproitic component in the high-K calc-alkaline volcanic rocks of the Capraia Island, Tuscan Magmatic Province: evidence from clinopyroxene crystal chemical data. *Periodico Mineralogia*, **75**, 75–94.

Chopin, C. 1984. Coesite and pure pyrope in high grade blueschists of the Western Alps, a first record and some consequences. *Contributions to Mineralogy and Petrology*, **86**, 107–118, https://doi.org/10.1007/BF00381838

Cifelli, F., Mattei, M. and Rossetti, F. 2007. Tectonic evolution of arcuate mountain belts on top of a retreating subduction slab: the example of the Calabrian Arc. *Journal of Geophysical Research*, **112**, B09101, https://doi.org/10.1029/2006JB004848

Cifelli, F., Mattei, M. and Porreca, M. 2008. New paleomagnetic data from Oligocene–upper Miocene sediments in the Rif chain (northern Morocco): insights on the Neogene tectonic evolution of the Gibraltar arc. *Journal of Geophysical Research*, **113**, B02104, https://doi.org/10.1029/2007JB005271

Civetta, L., Orsi, G., Scandone, P. and Pece, R. 1978. Eastward migration of the Tuscan Anatectic magmatism due to anticlockwise rotation of the Apennines. *Nature*, **276**, 604–606, https://doi.org/10.1038/276604a0

Comas, M.C., Platt, J.P., Soto, J.I. and Watts, A.B. 1999. The origin and tectonic history of the Alborán Basin: insights from ODP Leg 161 results. *In*: Zahn, R., Comas, M.C. and Klaus, A. (eds) *Proceedings of the Ocean Drilling Program, Scientific Results*. Ocean Drilling Program, **161**, 555–580, https://doi.org/10.2973/odp.proc.sr.161.262.1999

Conceição, R.V. and Green, D.H. 2004. Derivation of potassic (shoshonitic) magmas by decompressing melting of phlogopite + pargasite lherzolite. *Lithos*, **72**, 209–229, https://doi.org/10.1016/j.lithos.2003.09.003

Conticelli, S. 1998. The effects of crustal contamination on ultrapotassic magmas with lamproitic affinity: mineralogical, geochemical and isotope data from the Torre Alfina lavas and xenoliths, Central Italy. *Chemical Geology*, **149**, 51–81, https://doi.org/10.1016/S0009-2541(98)00038-2

Conticelli, S. and Peccerillo, A. 1990. Petrological significance of high-pressure ultramafic xenoliths from ultrapotassic rocks of Central Italy. *Lithos*, **24**, 305–322, https://doi.org/10.1016/0024-4937(89)90050-9

Conticelli, S. and Peccerillo, A. 1992. Petrology and geochemistry of potassic and ultrapotassic alkalic volcanism in Central Italy: petrogenesis and interferences on the mantle source. *Lithos*, **28**, 21–240, https://doi.org/10.1016/0024-4937(92)90008-M

Conticelli, S., Manetti, P. and Menichetti, S. 1992. Petrology, chemistry, mineralogy and Sr isotopic features of Pliocenic Orendites from South Tuscany: implications on their genesis and evolutions. *European Journal of Mineralogy*, **4**, 1359–1375, https://doi.org/10.1127/ejm/4/6/1359

Conticelli, S., Bortolotti, V., Principi, G., Laurenzi, M.A., Vaggelli, G. and D'Antonio, M. 2001. Petrology, mineralogy and geochemistry of a mafic dyke from Monte Castello, Elba Island, Italy. *Ofioliti*, **26**, 249–262, https://doi.org/10.4454/ofioliti.v26i2a.149

Conticelli, S., D'Antonio, M., Pinarelli, L. and Civetta, L. 2002. Source contamination and mantle heterogeneity in the genesis of Italian potassic and ultrapotassic volcanic rocks: Sr-Nd-Pb isotope data from Roman province and Southern Tuscany. *Mineralogy and Petrology*, **74**, 189–222, https://doi.org/10.1007/s007100200004

Conticelli, S., Carlson, R.W., Widow, E. and Serri, G. 2007. Chemical and isotopic composition (Os, Pb, Nd, and Sr) of Neogene to Quaternary calc-alkaline, shoshonitic, and ultrapotassic mafic rocks from the Italian peninsula: inferences on the nature of their mantle sources. *In*: Beccaluva, L., Bianchini, G. and Wilson, M. (eds) *Cenozoic Volcanism in the Mediterranean Area*. Geological Society of America, Special Papers, **418**, 171–202, https://doi.org/10.1130/2007.2418(09)

Conticelli, S., Guarnieri, L. *et al*. 2009. Trace elements and Sr-Nd-Pb isotopes of K-rich, shoshonitic, and calc-alkaline magmatism of the Western Mediterranean Region: genesis of ultrapotassic to calcalkaline magmatic associations in a post-collisional geodynamic setting. *Lithos*, **107,** 68–92, https://doi.org/10.1016/j.lithos.2008.07.016

Conticelli, S., Avanzinelli, R., Marchionni, S., Tommasini, S. and Melluso, L. 2011. Sr–Nd–Pb isotopes from the Radicofani Volcano, Central Italy: constraints on heterogeneities in a veined mantle responsible for the shift from ultrapotassic shoshonite to basaltic andesite magmas in a post-collisional setting. *Mineralogy and Petrology*, **103**, 123–148, https://doi.org/10.1007/s00710-011-0161-y

Conticelli, S., Avanzinelli, R., Poli, G., Braschi, E. and Giordano, G. 2013. Shift from lamproite-like to leucititic rocks. Sr–Nd–Pb isotope data from the Monte Cimino dome complex and the Vico stratovolcano, Central Italy. *Chemical Geology*, **353**, 246–266, https://doi.org/10.1016/j.chemgeo.2012.10.018

Conticelli, S., Avanzinelli, R., Ammannati, E. and Casalini, M. 2015. The role of carbon from recycled sediments in the origin of ultrapotassic igneous rocks in the Central Mediterranean. *Lithos*, **232**, 174–196, https://doi.org/10.1016/j.lithos.2015.07.002

Cross, W. 1897. Igneous rocks of the Leucite Hills and Pilot Butte, Wyoming. *American Journal of Science*, **14**, 115–141, https://doi.org/10.2475/ajs.s4-4.20.115

Cvetković, V., Prelević, D., Downes, H., Jovanović, M., Vaselli, O. and Pécskay, Z. 2004*a*. Origin and geodynamic significance of Tertiary post-collisional basaltic magmatism in Serbia (Central Balkan Peninsula). *Lithos*, **73**, 161–186, https://doi.org/10.1016/j.lithos.2003.12.004

Cvetković, V., Downes, H., Prelević, D., Jovanović, M. and Lazarov, M. 2004*b*. Characteristics of the lithospheric mantle beneath East Serbia inferred from ultramafic xenoliths in Palaeogene basanites. *Contributions to Mineralogy and Petrology*, **148**, 335–357, https://doi.org/10.1007/s00410-004-0607-x

Dal Piaz, G.V., Venturelli, G. and Scolari, A. 1979. Calc-alkaline to ultrapotassic postcollisional volcanic activity in the internal northwestern Alps. *Memorie della Società Geologica Università di Padova*, **32**, 4–16.

Dallai, L, Bianchini, G, Avanzinelli, R, Natali, C. and Conticelli, S. 2019. Heavy oxygen recycled into the lithospheric mantle. *Scientific Reports*, **9**, 1–7, https://doi.org/10.1038/s41598-019-45031-3

Davies, G.R., Stolz, A.J., Mahotkin, I.L., Nowell, G.M. and Pearson, D.G. 2006. Trace element and Sr–Pb–Nd–Hf isotope evidence for ancient, fluid-dominated enrichment of the source of Aldan Shield lamproites. *Journal of Petrology*, **47**, 1119–1146, https://doi.org/10.1093/petrology/egl005

De Yarza, R.A. 1895. Rocha eruptiva de Fortuna (Provincia de Murcia). *Boll Comm Mapa Geol Espana*, **20**, 349–353.

Dercourt, J., Zonenshein, L.P. *et al*. 1986. Geological evolution of the Tethys belt from the Atlantic to the Pamirs since the Lias. *Tectonophysics*, **123**, 241–315, https://doi.org/10.1016/0040-1951(86)90199-X

Dewey, J.F., Helman, M.L., Turco, E., Hutton, D.H.W. and Knott, S.D. 1989. Kinematics of the Western Mediterranean. *Geological Society, London, Special Publications*, **45**, 265–283, https://doi.org/10.1144/GSL.SP.1989.045.01.15

D'Orazio, M., Laurenzi, M.A. and Villa, I.M. 1991. $^{40}Ar/^{39}Ar$ dating of a shoshonitic lava flow of the Radicofani volcanic center (Southern Tuscany). *Acta Vulcanologica*, **1**, 63–67.

Doglioni, C., Agostini, S., Crespi, M., Innocenti, F., Manetti, P., Riguzzi, F. and Savascin, Y. 2002. On the extension in western Anatolia and the Aegean Sea. *Journal of the Virtual Explorer*, **8**, 169–183, https://doi.org/10.3809/jvirtex.2002.00049

Duggen, S., Hoernle, K., Van Den Bogaard, P. and Garbe-Schonberg, D. 2005. Post-collisional transition from subduction-to intraplate-type magmatism in the westernmost Mediterranean: evidence for continental-edge delamination of subcontinental lithosphere. *Journal of Petrology*, **46**, 1155–1201, https://doi.org/10.1093/petrology/egi013

Duggen, S., Höernle, K. *et al*. 2008. Geochemical zonation of the Miocene Alborán Basin volcanism (westernmost Mediterranean): geodynamic implications. *Contributions to Mineralogy and Petrology*, **156**, 577–593, https://doi.org/10.1007/s00410-008-0302-4

Edgar, A.D. and Mitchell, R.H. 1997. Ultra-high pressure–temperature melting experiments on an SiO_2-rich lamproite from Smokey Butte, Montana, derivation of siliceous lamproite magmas from enriched source deep in the continental mantle. *Journal of Petrology*, **38**, 457–477, https://doi.org/10.1093/petroj/38.4.457

Ersoy,Y. and Helvaci, C. 2007. Stratigraphy and geochemical features of the Early Miocene bimodal (ultrapotassic and calc-alkaline) volcanic activity within the NE-trending Selendi Basin, Western Anatolia, Turkey. *Turkish Journal of Earth Sciences*, **16**, 117–139

Ewart, A. 1982. The mineralogy and petrology of Tertiary-Recent orogenic volcanic rocks: with special reference to the andesitic-basaltic compositional range. *In*: Thorpe, R.S. (ed.) *Andesites: Orogenic Andesites and Related Rocks*. John Wiley and Sons, New York, https://doi.org/10.1007/BF00389774

Faccenna, C., Piromallo, C., Crespo-Blanc, A., Jolivet, L. and Rossetti, F. 2004. Lateral slab deformation and the origin of the western Mediterranean arcs. *Tectonics*, **23**, TC1012, https://doi.org/10.1029/2002TC001488

Faccenna, C., Becker, T.W. *et al*. 2014. Mantle dynamics in the Mediterranean, *Reviews of Geophysics*, **52**, https://doi.org/10.1002/ 2013RG000444

Festa, A., Balestro, G., Borghi, A., De Caroli, S. and Succo, A. 2020. The role of structural inheritance in continental break-up and exhumation of Alpine Tethyan mantle (Canavese Zone, Western Alps). *Geoscience Frontiers*, **11**, 167–188, https://doi.org/10.1016/j.gsf.2018.11.007

Foley, S.F. 1990. A review and assessment of experiments on kimberlites, lamproites and lamprophyres as a guide to their origin. *Proceedings Indian Academy of Sciences, Earth Science Reviews*, **99**, 77–80, https://doi.org/10.1007/BF02871896

Foley, S.F. 1992. Vein-plus-wall-rock melting mechanisms in the lithosphere and the origin of potassic alkaline magmas. *Lithos*, **28**, 435–453, https://doi.org/10.1016/0024-4937(92)90018-T

Foley, S.F. 1993. An experimental study of olivine lamproite – first results from the diamond stability field. *Geochimica et Cosmochimica Acta*, **57**, 483–489, https://doi.org/10.1016/0016-7037(93)90448-6

Foley, S. and Jenner, G. 2004. Trace element partitioning in lamproitic magmas - the Gaussberg olivine leucitite. *Lithos*, **75**, 19–38, https://doi.org/10.1016/j.lithos.2003.12.020

Foley, S.F. and Venturelli, G. 1989. High-K_2O rocks with high MgO, high SiO_2, affinities. *In*: Crawford, A.J. (ed.) *Boninites and Related Rocks*. Unwin Hyman, London, 72–88.

Foley, S.F., Venturelli, G., Green, D.H. and Toscani, L. 1987. The ultrapotassic rocks: characteristics, classification and constraints for petrogenetic models. *Earth-Science Reviews*, **24**, 81–134, https://doi.org/10.1016/0012-8252(87)90001-8

Foley, S.F., Prelević, D., Rehfeldt, T. and Jacob, D.E. 2013. Minor and trace elements in olivines as probes into early igneous and mantle melting processes. *Earth and Planetary Science Letters*, **363**, 181–191, https://doi.org/10.1016/j.epsl.2012.11.025

Francalanci, L., Innocenti, F., Manetti, P. and Savasçin, M.Y. 2000. Neogene alkaline volcanism of the Afyon-Isparta area, Turkey: petrogenesis and geodynamic implications. *Mineralogy and Petrology*, **70**, 285–312, https://doi.org/10.1007/s007100070007

Franz, L., Becker, K.-P., Kramer, W. and Herzig, P. 2002. Metasomatic mantle xenoliths from the Bismark

Microplate (Papua New Guinea) - thermal evolution, geochemistry and extent of slab-induced metasomatism. *Journal of Petrology*, **43**, 315–343, https://doi.org/10.1093/petrology/43.2.315

Fraser, K.J., Hawkesworth, C.J., Erlank, A.J., Mitchell, R.H. and Scott-Smith, B.H. 1985. Sr, Nd and Pb isotope and minor element geochemistry of lamproites and kimberlites. *Earth and Planetary Science Letters*, **76**, 57–70, https://doi.org/10.1016/0012-821X(85)90148-7

Fritschle, T., Prelević, D., Foley, S.F. and Jacob, D.E. 2013. Petrological characterization of the mantle source of Mediterranean lamproites: indications from major and trace elements of phlogopite. Chemical Geology, *Chemical Geology*, **353**, 267–279, https://doi.org/10.1016/j.chemgeo.2012.09.006

Gaetani, M., Dercourt, J. and Vrielynck, B. 2003. The peri-Tethys programme: achievements and results. *Episodes*, **26,** 79–93, https://doi.org/10.18814/epiiugs/2003/v26i2/002

Gagnevin, D., Waight, T.E., Daly, J.S., Poli, G. and Conticelli, S. 2007. Insights into magmatic evolution and recharge history in Capraia Volcano (Italy) from chemical and isotopic zoning in plagioclase phenocrysts. *Journal of Volcanology and Geothermal Research*, **168**, 28–54, https://doi.org/10.1016/j.jvolgeores.2007.07.018

Gale, A., Dalton, C.A., Langmuir, C.H., Su, Y. and Schilling, J.G. 2013. The mean composition of ocean ridge basalts. *Geochemistry Geophysics Geosystems*, **14**, 489–518, https://doi.org/10.1029/2012GC004334

Gao, Y., Hou, Z., Kamber, B.S., Wei, R., Meng, X. and Zhao, R. 2007. Lamproitic rocks from a continental collision zone: evidence for recycling of subducted Tethyan oceanic sediments in the mantle beneath Southern Tibet. *Journal of Petrology*, **48**, 729–752, https://doi.org/10.1093/petrology/egl080

Gasparon, M., Rosenbaum, G., Wijbrans, J. and Manetti, P. 2009. The transition from subduction arc to slab tearing: evidence from Capraia Island, northern Tyrrhenian Sea. *Journal of Geodynamics*, **47**, 30–38, https://doi.org/10.1016/j.jog.2008.06.004

Green, T., Blundy, J., Adam, J. and Yaxley, G. 2000. SIMS determination of trace element partition coefficients between garnet, clinopyroxene and hydrous basaltic liquids at 2–7.5 Gpa and 1080–1200C. *Lithos*, **53**, 165–187, https://doi.org/10.1016/S0024-4937(00)00023-2

Grégoire, M., McInnes, B.I.A. and O'Reilley, S.Y. 2001. Hydrous metasomatism of oceanic subarc mantle, Lihir, Papua New Guinea – Part 2. Trace element characteristics of slab-derived fluids. *Lithos*, **59**, 91–108, https://doi.org/10.1016/S0024-4937(01)00058-5

Hart, S.R. 1984. A large-scale isotope anomaly in the Southern Hemisphere mantle. *Nature*, **309**, 753–757, https://doi.org/10.1038/309753a0

Hermann, J. and Rubatto, D. 2009. Accessory phase control on the trace element signature of sediment melts in subduction zones. *Chemical Geology*, **265**, 512–526, https://doi.org/10.1016/j.chemgeo.2009.05.018

Horvath, F. and Berckheimer, H. 1982. Mediterranean backarc-basins. *In*: Berckheimer, H. and Hsü, K. (eds) *Alpine-Mediterranean-Geodynamics*. AGU Geodynamics Series, 141–163, https://doi.org/10.1029/GD007p0141

Hunziker, J.C. 1974. Rb–Sr age determination and the Alpine tectonic history of the Western Alps. *Memorie Istituto Geologia e Mineralogia Università di Padova*, **31**, 1–54, https://phaidra.cab.unipd.it/o:450775

Ilic, A., Neubauer, F. and Handler, R. 2005. Late Paleozoic–Mesozoic tectonics of the Dinarides revisited: implications from 40Ar/39Ar dating of detrital white micas. *Geology*, **33**, 233–236, https://doi.org/10.1130/G20979.1

Innocenti, F., Agostini, S., Di Vincenzo, G., Doglioni, C., Manetti, P., Savaşçin, M.Y. and Tonarini, S. 2005. Neogene and Quaternary volcanism in Western Anatolia: magma sources and geodynamic evolution. *Marine Geology*, **221**, 397–421, https://doi.org/10.1016/j.margeo.2005.03.016

Irving, A.J. and Kuehner, S.M. 1998. Petrology and geochemistry of the Ruby Slipper lamproite, western Montana: a leucite-bearing, ultrapotassic magma in an Eocene continental arc. *International Kimberlite Conference, Cape Town Extended Abstracts*, **7**, 349–351, https://doi.org/10.29173/ikc2731

Jaques, A.L. and Foley, S.F. 2018. Insights into the petrogenesis of the West Kimberley lamproites from trace elements in olivine. *Mineralogy and Petrology*, **112**, S519–S537, https://doi.org/10.1007/s00710-018-0612-9

Jaques, A.L., Lewis, J.D. and Smith, C.B. 1986. The kimberlites and lamproites of Western Australia. *Geological Survey of Western Australia*, **132**, 1–268.

Jaques, A.L., O'Neill, H.S.C., Smith, C.B., Moon, J. and Chappell, B.W. 1990. Diamondiferous peridotite xenoliths from the Argyle (AK1) lamproite pipe, Western Australia. *Contributions to Mineralogy and Petrology*, **104**, 255–276, https://doi.org/10.1007/BF00321484

Johnson, M.C. and Plank, T. 1999. Dehydration and melting experiments constrain the fate of subducted sediments. *Geochemistry Geophysics Geosystems*, **1**, 1007, https://doi.org/10.1029/1999GC000014

Jolivet, L. and Brun, J.P. 2010. Cenozoic geodynamic evolution of the Aegean region. *International Journal of Earth Science*, **99**, 109–138, https://doi.org/10.1007/s00531-00008-00366-00534

Kessel, R., Schmidt, M.W., Ulmer, P. and Pettke, T. 2005. Trace element signature of subduction-zone fluids, melts and superficial liquids at 120–180 km depth. *Nature*, **437**, 724–727, https://doi.org/10.1038/nature03971

Kissel, C. and Laj, C. 1988. The Tertiary geodynamic evolution of the Aegean arc: a paleomagnetic reconstruction, *Tectonophysics*, **146**, 183–201, https://doi.org/10.1016/0040-1951(88)90090-X

Klimm, K., Blundy, J.D. and Green, T.H. 2008. Trace element partitioning and accessory phase saturation during H_2O-saturated melting of basalt with implications for subduction zone chemical fluxes. *Journal of Petrology*, **49**, 523–553, https://doi.org/10.1093/petrology/egn001

Kovács, I., Csontos, L., Szabó, C., Bali, E., Falus, G., Benedek, K. and Zajacz, Z. 2007. Paleogene–Early Miocene igneous rocks and geodynamics of the Alpine–Carpathian–Pannonian–Dinaric region: an integrated approach. *In*: Beccaluva, L., Bianchini, G. and Wilson, M. (eds) *Volcanism in the Mediterranean Area*.

Geological Society of America Special Papers, **418**, 93–112, https://doi.org/10.1130/2007.2418(05)

Krmíček, L., Romer, R.L., Ulrych, J., Glodny, J. and Prelević, D. 2016. Petrogenesis of orogenic lamproites of the Bohemian Massif: Sr–Nd–Pb–Li isotope constraints for Variscan enrichment of ultra-depleted mantle domains. *Gondwana Research*, **35**, 198–216, https://doi.org/10.1016/j.gr.2015.04.012

Krmíček, L., Romer, R.L., Cempírek, J., Gadas, P., Krmíčková, S. and Glodny, J. 2020. Petrographic and Sr–Nd–Pb–Li isotope characteristics of a complex lamproite intrusion from the Saxo-Thuringian Zone: a unique example of peralkaline mantle-derived melt differentiation. *Lithos*, **374**, 105735, https://doi.org/10.1016/j.lithos.2020.105735

Krummenacher, D. and Evernden, J.F. 1960. Determination d'age isotopique faites sur quelques roches des Alps par la méthode potassium-argon. *Schweizerische Mineralogische und Petrographische Mitteilungen*, **40**, 267–277.

Kuiper, K.F., Krijgsman, W., Garcés, M. and Wijbrans, J.R. 2006. Revised isotopic ($^{40}Ar/^{39}Ar$) age for the lamproite volcano of Cabezos Negros, Fortuna basin (eastern Betics, SE Spain). *Palaeogeography, Palaeoclimatology, Palaeoecology*, **238**, 53–63, https://doi.org/10.1016/j.palaeo.2006.03.017

Lambert, D.D., Shirey, S.B. and Bergman, S.C. 1995. Proterozoic lithospheric mantle source for the Prairie Creek lLamproites: Re–Os and Sm-Nd isotopic evidence. *Geology*, **23**, 273–276, https://doi.org/10.1130/0091-7613(1995)023<0273:PLMSFT>2.3.CO;2

Lonergan, L. and White, N. 1997. Origin of the Betic–Rif mountain Belt. *Tectonics*, **16**, 504–522, https://doi.org/10.1029/96TC03937

Lustrino, M., Agostini, S., Chalal, Y., Fedele, L., Stagno, V., Colombi, F. and Bouguerra, A. 2016. Exotic lamproites or normal ultrapotassic rocks? The Late Miocene volcanic rocks from Kef Hahouner, NE Algeria, in the frame of the circum-Mediterranean lamproites. *Journal of Volcanology and Geothermal Research*, **327**, 539–553, https://doi.org/10.1016/j.jvolgeores.2016.09.021

Malinverno, A. and Ryan, W.B.F. 1986. Extension in the Tyrrhenian Sea and shortening in the Apennines as result of arc migration driven by sinking of the lithosphere. *Tectonics*, **5**, 227–245, https://doi.org/10.1029/TC005i002p00227

Marchesi, C., Konc, Z., Garrido, C.J., Boschc, D., Hidas, K., Varas-Reus, M.I. and Acosta-Vigil, A. 2017. Multistage evolution of the lithospheric mantle beneath the westernmost Mediterranean: geochemical constraints from peridotite xenoliths in the eastern Betic Cordillera (SE Spain). *Lithos*, **276**, 75–89, https://doi.org/10.1016/j.lithos.2016.12.011

Martelli, M., Bianchini, G., Beccaluva, L. and Rizzo, A. 2011. Helium and argon isotopic compositions of mantle xenoliths from Tallante and Calatrava, Spain. *Journal of Volcanology and Geothermal Research*, **200**, 18–26, https://doi.org/10.1016/j.jvolgeores.2010.11.015

Martin, L.A.J., Hermann, J., Gauthiez-Putallaz, L., Whitne, D.L., Vitale Brovarone, A., Fornash, K.F. and Evans, N.J. 2014. Lawsonite geochemistry and stability-implication for trace element and water cycles in subduction zones. *Journal of Metamorphic Geology*, **32**, 455–478, https://doi.org/10.1111/jmg.12093

Martindale, M., Skora, S., Pickles, J., Elliott, T., Blundy, J. and Avanzinelli, R. 2013. High pressure phase relations of subducted volcaniclastic sediments from the west pacific and their implications for the geochemistry of Mariana arc magmas. *Chemical Geology*, **342**, 94–109, https://doi.org/10.1016/j.chemgeo.2013.01.015

Mascle, G.H., Tricart, P. *et al.* 2001. Evolution of the Sardinia Channel (Western Mediterranean): new constraints from a diving survey on Cornacya seamount off SE Sardinia. *Marine Geology*, **179**, 179–201, https://doi.org/10.1016/S0025-3227(01)00220-1

Mattei, M., Cifelli, F., Martín Rojas, I., Crespo Blanc, A., Comas, M., Faccenna, C. and Porreca, M. 2006. Neogene tectonic evolution of the Gibraltar Arc: new paleomagnetic constrains from the Betic chain. *Earth and Planetary Science Letters*, **250**, 522–540, https://doi.org/10.1016/j.epsl.2006.08.012

Mattei, M., Riggs, N.R. *et al.* 2014. Geochronology, geochemistry and geodynamics of the Cabo de Gata volcanic zone, Southeastern Spain. *Italian Journal of Geoscience*, **133**, 341–361, https://doi.org/10.3301/IJG.2014.44

McCulloch, M.T., Jaques, A.L., Nelson, D.R. and Lewis, J.D. 1983. Nd and Sr isotopes in kimberlites and lamproites from Western Australia: an enriched mantle origin. *Nature*, **302**, 400–403, https://doi.org/10.1038/302400a0

McDonough, W.F. 1990. Constraints on the composition of the continental lithospheric mantle. *Earth and Planetary Science Letters*, **101**, 1–18, https://doi.org/10.1016/0012-821X(90)90119-I

McKenzie, D.P. 1970. Plate tectonics of the Mediterranean region. *Nature*, **226**, 239–243, https://doi.org/10.1038/226239a0

Melzer, S. and Foley, S.F. 2000. Phase relations and fractionation sequences in potassic magma series modelled in the system $CaMgSi_2O_6$-$KAlSiO_4$-Mg_2SiO_4-F_2O^{-1} at 1 bar to 18 kbar. *Contributions to Mineralogy and Petrology*, **138**, 186–197, https://doi.org/10.1007/s004100050017

Miller, C., Schuster, R., Klotzli, U., Frank, W. and Purtscheller, F. 1999. Post-collisional potassic and ultrapotassic magmatism in SW Tibet: geochemical and Sr-Nd-Pb-O isotopic constraints for mantle source characteristics and petrogenesis. *Journal of Petrology*, **40**, 1399–1424, https://doi.org/10.1093/petroj/40.9.1399

Mirnejad, H. and Bell, K. 2006. Origin and source evolution of the Leucite Hills lamproites: evidence from Sr–Nd–Pb–O isotopic compositions. *Journal of Petrology*, **47**, 2463–2489, https://doi.org/10.1093/petrology/egl051

Mitchell, R.H. 2020. Igneous rock associations 26. lamproites, exotic potassic alkaline rocks: a review of their nomenclature, characterization and origins. *Geoscience Canada*, **47**, 119–142, https://doi.org/10.12789/geocanj.2020.47.162

Mitchell, R.H. and Bergman, S.C. 1991. *Petrology of Lamproites*. Plenum Publishing Corporation, New York.

Murphy, D.T., Collerson, K.D. and Kamber, B.S. 2002. Lamproites from Gaussberg Antarctica: possible transition zone melts of Archaean subducted sediments.

Journal of Petrology, **43**, 981–1001, https://doi.org/10.1093/petrology/43.6.981

Nelson, D.R. 1989. Isotopic characteristics and petrogenesis of the lamproites and kimberlites of central West Greenland. *Lithos*, **22**, 265–274, https://doi.org/10.1016/0024-4937(89)90029-7

Nelson, D.R. 1992. Isotopic characteristics of potassic rocks: evidence for the involvement of subducted sediments in magma genesis. *Lithos*, **28**, 403–420, https://doi.org/10.1016/0024-4937(92)90016-R

Nelson, D.R., McCulloch, M.T. and Sun, S.-S. 1986. The origins of ultrapotassic rocks as inferred from Sr, Nd and Pb isotopes. *Geochimica et Cosmochimica Acta*, **50**, 231–245, https://doi.org/10.1016/0016-7037(86)90172-9

Nicoletti, M. 1969. Datazioni argon potassio di alcune vulcaniti delle Regioni vulcaniche Cimina e Vicana. *Periodico Mineralogia*, **38**, 1–20.

Nicoletti, M., Petrucciani, C., Piro, M. and Trigila, R. 1981. Nuove datazioni Vulsinee per uno schema di evoluzione dell'attività vulcanica: Il quadrante nord-occidentale. *Periodico Mineralogia*, **48**, 153–165.

Okay, A.I. 2008. Geology of Turkey: a synopsis. *Anschnitt*, **21**, 19–42.

Okay, A.I., Satir, M. and Siebel, W. 2006. Pre-Alpide Palaeozoic and Mesozoic orogenic events in the Eastern Mediterranean region. *Geological Society, London, Memoirs*, **32**, 389–405, https://doi.org/10.1144/GSL.MEM.2006.032.01.23

Osann, A. 1906. *Über einige Alkaligestein aus Spanien: Festschrift Rosenbusch*. *In*: Wülfing, E.A. (*Herausgeber*): *Festschrift Harry Rosenbusch*, Schweizerbart, Stuttgart, 283–301.

Owen, J.P. 2008. Geochemistry of lamprophyres from the Western Alps, Italy: implications for the origin of an enriched isotopic component in the Italian mantle. *Contributions to Mineralogy and Petrology*, **155**, 341–362, https://doi.org/10.1007/s00410-007-0246-0

Pasquaré, G., Chiesa, S., Vezzoli, L. and Zanchi, A. 1983. Evoluzione paleogeografica e strutturale di parte della Toscana meridionale a partire dal Miocene superiore. *Memorie della Società Geologica Italiana*, **25**, 145–157.

Peccerillo, A. and Martinotti, G. 2006. The Western Mediterranean lamproitic magmatism: origin and geodynamic significance. *Terra Nova*, **18**, 109–117, https://doi.org/10.1111/j.1365-3121.2006.00670.x

Peccerillo, A., Poli, G. and Serri, G. 1988. Petrogenesis of orenditic and kamafugitic rocks from Central Italy. *Canadian Mineralogist*, **26**, 45–65.

Pérez-Valera, L.A., Rosenbaum, G., Sánchez-Gómez, M., Azor, A., Fernández-Soler, J.M., Pérez-Valera, F. and Vasconcelos, P.M. 2013. Age distribution of lamproites along the Socovos Fault (southern Spain) and lithospheric scale tearing. *Lithos*, **180–181**, 252–263, https://doi.org/10.1016/j.lithos.2013.08.016

Perini, G., Tepley, F.J., III, Davidson, J.P. and Conticelli, S., 2003. The origin of K-feldspar megacrysts hosted in alkaline potassic rocks: track for low scale mantle heterogeneity. *Lithos*, **66**, 223–240, https://doi.org/10.1016/S0024-4937(02)00221-9

Pfiffner, O.A. 2021. The Alps. *In*: Alderton, D. and Elias, S.A. (eds) *Encyclopedia of Geology*. 2nd edn, Academic Press, 420–435, https://doi.org/10.1016/B978-0-12-409548-9.02774-3

Plank, T. 2005. Constraints from thorium/lanthanum on sediment recycling at subduction zones and the evolution of the continents. *Journal of Petrology*, **46**, 921–944, https://doi.org/10.1093/petrology/egi005

Plank, T. and Langmuir, C.H. 1998. The chemical composition of subducting sediments and its consequence for the crust and mantle. *Chemical Geology*, **145**, 325–394, https://doi.org/10.1016/S0009-2541(97)00150-2

Platt, P., Argles, T.W., Carter, A., Kelley, S.P., Whitehouse, M.J. and Lonergan, L. 2003. Exhumation of the Ronda peridotite and its crustal envelope: constraints from thermal modelling of a P–T–time array. *Journal of the Geological Society*, **160**, 655–676, https://doi.org/10.1144/0016-764902-108

Platt, J.P., Behr, W.M., Johanesen, K. and Williams, J.R. 2013. The Betic-Rif Arc and its orogenic hinterland: a review. *Annual Review of Earth and Planetary Science Letters*, **41**, 14.1–14.45, https://doi.org/10.1146/annurev-earth-050212-123951

Prelević, D. and Foley, S.F. 2007. Accretion of arc-oceanic lithospheric mantle in the Mediterranean: evidence from extremely high-Mg olivines and Cr-rich spinel inclusions from lamproites. *Earth and Planetary Science Letters*, **256**, 120–135, https://doi.org/10.1016/j.epsl.2007.01.018

Prelević, D., Foley, S.F. and Cvetkovic, V. 2007. A review of petrogenesis of Mediterranean Tertiary lamproites: a perspective from the Serbian ultrapotassic province. *Special Papers-Geological Society of America*, **418**, 113, https://doi.org/10.1130/2007.2418(06)

Prelević, D., Foley, S.F., Cvetković, V. and Romer, R.L. 2004. Origin of minette by mixing of lamproite and dacite magmas in Veliki Majdan, Serbia. *Journal of Petrology*, **45**, 759–792, https://doi.org/10.1093/petrology/egg109

Prelević, D., Foley, S.F., Romer, R.L., Cvetković, V. and Downes, H. 2005. Tertiary ultrapotassic volcanism in Serbia: constraints on petrogenesis and mantle source characteristics. *Journal of Petrology*, **46**, 1443–1487, https://doi.org/10.1093/petrology/egi022

Prelević, D., Foley, S.F., Romer, R.L. and Conticelli, S. 2008. Mediterranean Tertiary lamproites derived from multiple source components in postcollisional geodynamics. *Geochimica et Cosmochimica Acta*, **72**, 2125–2156, https://doi.org/10.1016/j.gca.2008.01.029

Prelević, D., Stracke, A., Foley, S.F., Romer, R.L. and Conticelli, S. 2010. Hf isotope compositions of Mediterranean lamproites: mixing of melts from asthenosphere and crustally contaminated mantle lithosphere. *Lithos*, **119**, 297–312, https://doi.org/10.1016/j.lithos.2010.07.007

Prelević, D., Akal, C., Foley, S.F., Romer, R.L., Stracke, A. and Van Den Bogaard, P. 2012. Ultrapotassic mafic rocks as geochemical proxies for post-collisional dynamics of orogenic lithospheric mantle: the case of Southwestern Anatolia, Turkey. *Journal of Petrology*, **53**, 1019–1055, https://doi.org/10.1093/petrology/egs008

Prelević, D., Akal, C., Romer, R.L., Mertz-Kraus, R. and Helvacı, C. 2015. Magmatic response to slab tearing: constraints from the Afyon Alkaline Volcanic Complex, Western Turkey. *Journal of Petrology*, **56**, 527–562, https://doi.org/10.1093/petrology/egv008

Quick, J.E., Sinigoi, S. and Mayer, A. 1995. Emplacement of mantle peridotite in the lower continental crust, Ivrea-Verbano zone, Northwest Italy. *Geology*, **23**, 739–742, https://doi.org/10.1130/0091-7613(1995)023<0739:EOMPIT>2.3.CO;2

Rampone, E., Vissers, R.L.M., Poggio, M., Scambelluri, M. and Zanetti, A. 2010. Melt migration and intrusion during exhumation of the Alboran lithosphere: the Tallante Mantle Xenolith Record (Betic Cordillera, SE Spain) *Journal of Petrology*, **51**, 295–325, https://doi.org/10.1093/petrology/egp061

Ribeiro, A., Munhá, J. *et al*. 2007. Geodynamic evolution of the SW Europe Variscides. *Tectonics*, **26**, https://doi.org/10.1029/2006TC002058

Rizzo, G., Piluso, E. and Morten, L. 2001. Phlogopite from the Serre ultramafic rocks, Central Calabria, Southern Italy. *European Journal of Mineralogy*, **13**, 1139–1151, https://doi.org/10.1127/0935-1221/2001/0013-1139

Robertson, A.H.F., Parlak, O. and Ustaömer, T. 2012. Overview of the Palaeozoic–Neogene evolution of Neotethys in the Eastern Mediterranean region (southern Turkey, Cyprus, Syria) *Petroleum Geoscience*, **18**, 381–404, https://doi.org/10.1144/petgeo2011-091 https://doi.org/10.1144/petgeo2011-091

Rock, N.M.S. 1987. The nature and origin of lamprophyres: an overview *Geological Society of London, Special Publication*, **30**, 191–226, https://doi.org/10.1144/GSL.SP.1987.030.01.09

Royden, L., Patacca, E. and Scandone, P. 1987. Segmentation and configuration of subducted lithosphere in Italy: an important control on thrust-belt and foredeep-basin evolution. *Geology*, **15**, 714–717, https://doi.org/10.1130/0091-7613(1987)15<714:SACOSL>2.0.CO;2

Rudnick, R.L. and Gao, S. 2003. Composition of the continental crust. *In*: Rudnick, R.L. (ed.) *The Crust*. Treatise on Geochemistry, Elsevier-Pergamon, Oxford, **3**. 1–64, https://doi.org/10.1016/B0-08-043751-6/03016-4

Schmid, S.M., Fügenschuh, B., Kissling, E. and Schuster, R. 2004. Tectonic map and overall architecture of the Alpine orogen. *Eclogae geologicae Helvetiae*, **97**, 93–117, https://doi.org/10.1007/s00015-004-1113-x

Schreyer, W., Massonne, H.J. and Chopin, C. 1987. Continental crust subducted to depths near 100 kmimplications for magma and fluid genesis in collision zones. *In*: Mysen, B.O. (ed.) *Magmatic Processes: Physicochemical principles*. Geochemical Society, America, Special Publications, **1**, 155–163.

Scotese, C.R. 2004. A continental drift flipbook. *Journal of Geology*, **112**, 729–741, https://doi.org/10.1086/424867

Sekine, T. and Wyllie, P.J. 1982. Phase relationships in the system $KAlSiO_4$–Mg_2SiO_4–SiO_2–H_2O as a model for hybridization between hydrous siliceous melts and peridotite. *Contributions to Mineralogy and Petrology*, **79**, 368–374, https://doi.org/10.1007/BF01132066

Sengör, A.M.C. 1979. Mid-Mesozoic closure of Permo-Triassic Tethys and its implications. *Nature*, **279**, 590–593, https://doi.org/10.1038/279590a0

Shimizu, Y., Arai, S., Morishita, T. and Ishida, Y. 2005. Geochemical signature of the quartz diorite vein in mantle peridotite xenolith from Tallante, SE Spain: laser-ablation ICP-MS analysis. *Ofioliti*, **30**, 263–264, https://doi.org/10.4454/ofioliti.v30i2.309

Skora, S. and Blundy, J. 2010. High-pressure hydrous phase relations of radiolarian clay and implications for the involvement of subducted sediment in arc magmatism. *Journal of Petrology*, **51**, 2211–2243, https://doi.org/10.1093/petrology/egq054

Skora, S., Blundy, J.D., Brooker, R.A., Green, E.C.R., de Hoog, J.C.M. and Connolly, J.A.D. 2015. Hydrous phase relations and trace element partitioning behaviour in calcareous sediments at subduction zone conditions. *Journal of Petrology*, **56**, 953– 980, https://doi.org/10.1093/petrology/egv024

Soder, C.G. and Romer, R.L. 2018. Post-collisional potassic-ultrapotassic magmatism of the Variscan Orogen: implications for mantle metasomatism during continental subduction. *Journal of Petrology*, **59**, 1007–1034, https://doi.org/10.1093/petrology/egy053

Spandler, C., Hermann, J., Arculus, R. and Mavrogenes, J. 2003. Redistribution of trace elements during prograde metamorphism from lawsonite blueschist to eclogite facies; implications for deep subduction-zone processes. *Contributions to Mineralogy and Petrology*, **146**, 205–222, https://doi.org/10.1007/s00410-003-0495-5

Stampfli, G.M. 2000. Tethyan Oceans. *Geological Society, London, Special Publications*, **173**, 1–23, https://doi.org/10.1144/GSL.SP.2000.173.01.01

Stampfli, G.M. and Borel, G.D. 2002. A plate tectonic model for the Paleozoic and Mesozoic constrained by dynamic plate boundaries and restored synthetic oceanic isochrons. *Earth and Planetary Science Letters*, **196**, 17–33, https://doi.org/10.1016/S0012-821X(01)00588-X

Stampfli, G.M., Mosar, J., Favre, P., Pillevuit, A. and Vannay, J.C. 2001. Permo–Mesozoic evolution of the Western Tethys realm: the Neo-Tethys East Mediterranean Basin connection. *In*: Ziegler, P.A. (ed.) *Peri-Tethys Memoir 6: Peri-Tethyan Rift/Wrench Basins and Passive Margins*. Memories de Museé Historie Naturelle Paris, **186**, 51–108, http://pascal-francis.inist.fr/vibad/index.php?action=getRecordDetail&idt=13427443

Stocklin, J. 1974. Possible ancient continental margins in Iran. *In*: Burk, C. and Drake, C. (eds) *The Geology of Continental Margins*. Springer, Berlin, 873–887, https://doi.org/10.1007/978-3-662-01141-6_64

Stracke, A., Bizimis, M. and Salters, V.J.M. 2003. Recycling oceanic crust: quantitative constraints. *Geochemistry, Geophysics, Geosystems*, **4**, https://doi.org/10.1029/2001GC000223

Straub, S.M., La Gatta, A.B., Martin-Del Pozzo, A.L. and Langmuir, C.H. 2008. Evidence from high-Ni olivines for a hybridized peridotite/pyroxenite source for orogenic andesites from the central Mexican volcanic belt. *Geochemistry Geophysics Geosystems*, **9**, Q03007, https://doi.org/10.1029/2007GC001583

Sun, S.-S. and McDonough, W.F. 1989. Chemical and isotopic systematics of Oceanic Basalts: implications for mantle composition and processes. *Geological Society, London, Special Publications*, **42**, 313–345, https://doi.org/10.1144/GSL.SP.1989.042.01.19

Taylor, H.P., Turi, B. and Cundari, A. 1984. $^{18}O/^{16}O$ and chemical relatioships in K-rich volcanic rocks from Australia, East Africa, Antarctica and San Venanzo-Cupaello, Italy. *Earth and Planetary Science Letters*, **69**, 263–276, https://doi.org/10.1016/0012-821X(84)90186-9

Terzić, M. and Svešnjikova, E.V. 1991. Age of leucite-bearing rocks in Yugoslavia. *Comptes Rendus des Sciences de la Société Serbe de Géologie*, **1987–1989**, 283–287.

Tommasini, S., Avanzinelli, R. and Conticelli, S. 2011. The Thorium/Lanthanum conundrum of the Tethyan realm lamproites: the role of recycled sediments and zoisite/lawsonite melting. *Earth and Planetary Science Letters*, **301**, 469–478, https://doi.org/10.1016/j.epsl.2010.11.023

Tubía, J.M., Cuevas, J. and Esteban, J.J. 2004. Tectonic evidence in the Ronda peridotites, Spain, for mantle diapirism related to delamination. *Geology*, **32**, 941–944, https://doi.org/10.1130/G20869.1

Turner, S., Platt, J.P., George, R.M.M., Kelley, S.P., Pearson, D.G. and Nowell, G.M. 1999. Magmatism associated with orogenic collapse of the Betic-Alboran domain, SE Spain. *Journal of Petrology*, **40**, 1011–1036, https://doi.org/10.1093/petroj/40.6.1011

Usui, T., Nakamura, E. and Helmstaedt, H.H. 2006. Petrology and geochemistry of eclogite xenoliths from the Colorado Plateau: implications for evolution of the subducted oceanic crust. *Journal of Petrology*, **47**, 929–964, https://doi.org/10.1093/petrology/egi101

Venturelli, G., Capedri, S., Di Battistini, G., Crawford, A., Kogarko, L.N. and Celestini, S. 1984*a*. The ultrapotassic rocks from southeastern Spain. *Lithos*, **17**, 37–54, https://doi.org/10.1016/0024-4937(84)90005-7

Venturelli, G., Thorpe, R.S., Dal Piaz, G.V., Del Moro, A. and Potts, P.J. 1984*b*. Petrogenesis of calc-alkaline, shoshonitic and associated ultrapotassic Oligocene volcanic rocks from Northwestern Alps, Italy. *Contribution to Mineralogy and Petrology*, **86**, 209–220, https://doi.org/10.1007/BF00373666

Vitale Brovarone, A., Alard, O., Beyssac, O., Martin, L. and Picatto, M. 2014. Lawsonite metasomatism and trace element recycling in subduction zones. *Journal of Metamorphic Geology*, **32**, 489–514, https://doi.org/10.1111/jmg.12074

Vollmer, R., Ogden, P., Schilling, J.G., Kingsley, R.H. and Waggoner, D.G. 1984. Nd and Sr isotopes in ultrapotassic volcanic rocks from the Leucite Hills, Wyoming. *Contributions to Mineralogy and Petrology*, **87**, 359–368, https://doi.org/10.1007/BF00381292

Von Blanckenburg, F., Kagami, H. *et al.* 1998. The origin of Alpine plutons along the Periadriatic Lineament. *Schweizerische Mineralogische und Petrographische Mitteilungen*, **78**, 55–66, https://doi.org/10.5169/seals-59274

Von Raumer, J., Stampfli, G., Borel, G. and Bussy, F. 2002. Organization of pre-Variscan basement areas at the north-Gondwanan margin. *International Journal of Earth Sciences*, **91**, 35–52, https://doi.org/10.1007/s005310100200

Wade, A. and Prider, R.T. 1940. The Leucite bearing-rocks of West Kimberley area, Western Australia. *Quarterly Journal of Geological Society London*, **96**, 39–98, https://doi.org/10.1144/GSL.JGS.1940.096.01-04.04

Wagner, C. and Velde, D. 1986. The mineralogy of K-richterite-bearing lamproite. *American Mineralogist*, **71**, 17–37.

Wang, Y. and Foley, S.F. 2020. The role of blueschist stored in shallow lithosphere in the generation of post- collisional orogenic magmas. *Journal of Geophysical Research: Solid Earth*, **125**, e2020JB019910, https://doi.org/10.1029/2020JB019910

Wang, Y., Prelević, D., Buhre, S. and Foley, S.F. 2017. Constraints on the sources of post-collisional K-rich magmatism: the roles of continental clastic sediments and terrigenous blueschists. *Chemical Geology*, **455**, 192–207, https://doi.org/10.1016/j.chemgeo.2016.10.006

Wang, Y., Prelević, D. and Foley, S.F. 2019. Geochemical characteristics of lawsonite blueschists in tectonic mélange from the Tavşanlı Zone, Turkey: potential constraints on the origin of Mediterranean potassium-rich magmatism. *American Mineralogist*, **104**, 724–743, https://doi.org/10.2138/am-2019-6818

Watts, A.B., Piatt, J.P. and Buhl, P. 1993. Tectonic evolution of the Alboran Sea basin. *Basin Research*, **5**, 153–177, https://doi.org/10.1111/j.1365-2117.1993.tb00063.x

Wheller, G.E., Varne, R., Foden, J.D. and Abbott, M.J. 1987. Geochemistry of Quaternary volcanism in the Sunda-Banda arc, Indonesia, and three-component genesis of island-arc basaltic magmas. *Journal of Volcanology and Geothermal Research*, **32**, 137–160, https://doi.org/10.1016/0377-0273(87)90041-2

Willbold, M. and Stracke, A. 2006. Trace element composition of mantle end-members: implications for recycling of oceanic and upper and lower continental crust. *Geochemistry, Geophysics, Geosystems*, **7**, https://doi.org/10.1029/2005GC001005

Woodland, A.B., Kornprobst, J., McPherson, E., Bodinier, J.L. and Menzies, M.A. 1996. Metasomatic interactions in the lithospheric mantle: petrologic evidence from the Lherz massif, French Pyrenees. *Chemical Geology*, **134**, 83–112, https://doi.org/10.1016/S0009-2541(96)00082-4

Yanev, Y., Boev, B. *et al.* 2008. Late Miocene to Pleistocene potassic volcanism in the Republic of Macedonia. *Mineralogy and Petrology*, **94**, 45–60, https://doi.org/10.1007/s00710-008-0009-2

Zanchetta, S., Berra, F., Zanchi, A., Bergomi, M., Caridroit, M., Nicora, A. and Heidarzadeh, G. 2013. The record of the Late Palaeozoic active margin of the Palaeotethys in NE Iran: constraints on the Cimmerian orogeny. *Gondwana Research*, **24**, 1237–1266, https://doi.org/10.1016/j.gr.2013.02.013

Zanchi, A., Zanchetta, S. *et al.* 2009. The Eo-Cimmerian (Late? Triassic) orogeny in north Iran. *Geological Society, London, Special Publications*, **312**, 31–55, https://doi.org/10.1144/SP312.3

Zanetti, A., Mazzucchelli, M., Rivalenti, G. and Vannucci, R. 1999. The Finero phlogopite-peridotite massif: an example of subduction-related metasomatism. *Contributions to Mineralogy and Petrology*, **134**, 107–122, https://doi.org/10.1007/s004100050472